Purification, Pharmacological Modulation, and Biochemical Characterization of Interactors of Endogenous Human γ-Secretase[†]

Edith Winkler,[‡] Scott Hobson,[§] Akio Fukumori,[‡] Birgit Dümpelfeld,[§] Thomas Luebbers,[||] Karlheinz Baumann,[||] Christian Haass,[‡] Carsten Hopf,[§] and Harald Steiner*[,‡]

Center for Integrated Protein Science Munich and Adolf-Butenandt-Institute, Department of Biochemistry, Laboratory for Neurodegenerative Disease Research, Ludwig-Maximilians-University, 80336 Munich, Germany, Cellzome AG, Meyerhofstrasse 1, 69117 Heidelberg, Germany, and Preclinical CNS Research, Pharmaceuticals Division, F. Hoffmann-La Roche Ltd., CH-4070 Basel, Switzerland

Received June 27, 2008; Revised Manuscript Received December 1, 2008

ABSTRACT: γ-Secretase is a unique intramembrane-cleaving protease complex, which cleaves the Alzheimer's disease-associated β-amyloid precursor protein (APP) and a number of other type I membrane proteins. Human γ-secretase consists of the catalytic subunit presenilin (PS) (PS1 or PS2), the substrate receptor nicastrin, APH-1 (APH-1a or APH-1b), and PEN-2. To facilitate in-depth biochemical analysis of γ-secretase, we developed a fast and convenient multistep purification procedure for the endogenous enzyme. The enzyme was purified from HEK293 cells in an active form and had a molecular mass of ~500 kDa. Purified γ-secretase was capable of producing the major amyloid-β peptide (Aβ) species, such as Aβ40 and Aβ42, from a recombinant APP substrate in physiological ratios. Aβ generation could be modulated by pharmacological γ-secretase modulators. Moreover, the Aβ42/Aβ40 ratio was strongly increased by purified PS1 L166P, an aggressive familial Alzheimer's disease mutant. Tandem mass spectrometry analysis revealed the consistent coisolation of several proteins with the known γ-secretase core subunits. Among these were the previously described γ-secretase interactors CD147 and TMP21 as well as other known interactors of these. Interestingly, the Niemann-Pick type C1 protein, a cholesterol transporter previously implicated in γ-secretase-mediated processing of APP, was identified as a major copurifying protein. Affinity capture experiments using a biotinylated transition-state analogue inhibitor of γ-secretase showed that these proteins are absent from active γ-secretase complexes. Taken together, we provide an effective procedure for isolating endogenous γ-secretase in considerably high grade, thus aiding further characterization of this pivotal enzyme. In addition, we provide evidence that the copurifying proteins identified are unlikely to be part of the active γ-secretase enzyme.

γ-Secretase is a member of the intramembrane-cleaving protease (I-CLiP)[1] family that comprises unusual proteolytic enzymes which cleave their substrates within the lipid bilayer of the membrane (*1*). Compared to other currently known I-CLiPs, γ-secretase is unique, as it requires complex formation of four proteins to constitute an active enzyme (*2*−*4*). The active complex is composed of four integral membrane proteins, the catalytic subunit presenilin (PS) (*5*−*12*), the substrate receptor nicastrin (NCT) (*13*), and two additional subunits, APH-1 (*14*) and PEN-2 (*15*), in a stoichiometry of 1:1:1:1 (*16*). A large number of γ-secretase substrates, which are all type I membrane proteins, have been identified (*17*). γ-Secretase substrate cleavage requires an initial cleavage in the extracellular domain by sheddases, which cleave in the proximity of the membrane and thus remove the bulk of the ectodomain. The remaining membrane-anchored C-terminal fragment (CTF) then becomes a substrate of γ-secretase, which cleaves within the hydrophobic transmembrane domain (TMD). This cleavage releases the intracellular domain (ICD) of the substrate into the cytosol and a small peptide into the extracellular space.

A major and critical substrate of γ-secretase is the β-amyloid precursor protein (APP), which has been implicated in Alzheimer's disease (AD) pathogenesis (*18*). The hydrophobic ~4 kDa amyloid β-peptide (Aβ), which is released upon cleavage of APP by β-secretase and γ-secretase, aggregates in the brain and becomes an invariant and defining neuropathological hallmark of AD. Following

[†] This work was supported by the Alzheimer Research Award of the Hans and Ilse Breuer Foundation (H.S.) and the Collaborative Research Center "Molecular Mechanisms of Neurodegeneration" (SFB 596) of the Deutsche Forschungsgemeinschaft (Ch.H. and H.S.).

* To whom correspondence should be addressed: Adolf-Butenandt-Institute, Department of Biochemistry, Schillerstrasse 44, 80336 Munich, Germany. Phone: (+49-89) 2180 75480. Fax: (+49-89) 2180 75415. E-mail: harald.steiner@med.uni-muenchen.de.

[‡] Ludwig-Maximilians-University.

[§] Cellzome AG.

[||] F. Hoffmann-La Roche Ltd.

[1] Abbreviations: Aβ, amyloid β-peptide; AICD, APP intracellular domain; AD, Alzheimer's disease; APP, β-amyloid precursor protein; CD-M6PR, cation-dependent mannose 6-phosphate receptor; CN-PAGE, colorless native PAGE; CTF, C-terminal fragment; DDM, *n*-dodecyl β-D-maltoside; FAD, familial Alzheimer's disease; GSI, γ-secretase inhibitor; GSM, γ-secretase modulator; ICD, intracellular domain; I-CLiP, intramembrane-cleaving protease; NCT, nicastrin; NPC1, Niemann-Pick type C1 protein; NSAID, nonsteroidal anti-inflammatory drug; NTF, N-terminal fragment; O/N, overnight; PPARα, peroxisome proliferator-activated receptor α; PS, presenilin; TMD, transmembrane domain.

10.1021/bi801204g CCC: $40.75
Published on Web 01/21/2009

cleavage of APP by β-secretase, which acts as a sheddase and removes the bulk of the APP ectodomain, the subsequently occurring γ-secretase cleavages release the APP ICD (AICD) from the ε-site and Aβ from the γ-site of the APP TMD. The latter cleavage is highly heterogeneous and produces Aβ species of different lengths. Although produced only in small amounts compared to the predominant Aβ40 variant, the Aβ42 variant is highly neurotoxic and believed to initiate the disease by triggering the amyloid cascade ultimately causing neuronal cell death and dementia (*18*). The central role of Aβ42 in the disease process is underscored by the mode of function of the vast majority of the rare, genetically inherited familial forms of AD (FAD). These mutations are predominantly found in PS, the catalytic subunit of γ-secretase, and to a lesser extent in its substrate, APP. All PS mutations associated with FAD, as well as the majority of the APP mutations, result in a shift of the cleavage specificity of γ-secretase and thereby an increase in the production of Aβ42 (*19*). The mutations in PS are located predominantly close to or within the TMDs, while the APP mutations that affect γ-secretase cleavage precision are located close to the γ-secretase cleavage sites in the APP TMD. With regard to the respective increase in the level of Aβ42, the effect of the FAD mutations ranges from being mild to severe. In the case of the very aggressive mutations, such as PS1 L166P (*20*) and other mutations (*21*), the production of Aβ42 exceeds that of Aβ40.

Because of its central role in the pathogenesis of AD, γ-secretase is an obvious and important potential drug target for the discovery and development of AD therapeutics. Although highly potent γ-secretase inhibitors (GSIs) have been known for some time, only one of them, LY450139, has entered late clinical phase (*22, 23*). Whether GSIs can be developed as AD therapeutics is still a matter of intense debate. The key complicating issue is the noted promiscuity of the γ-secretase enzyme. Most importantly, active site-directed inhibitors of γ-secretase also inhibit the cleavage of Notch, another crucial substrate of γ-secretase (*24*). Notch cleavage by γ-secretase releases the Notch ICD, which acts in the nucleus as a key transcriptional regulator controlling cell differentiation during development and adulthood (*25*). Not surprisingly, GSIs have been shown to cause severe side effects in the adult animal (*26, 27*), presumably via inhibition of the Notch signaling pathway (*28*). Despite recent evidence in transgenic mice suggesting that a therapeutic window between the APP and Notch substrates seems possible in vivo (*29*), it is at present unclear whether Notch-related side effects in humans can be mitigated by rational design of GSI compounds. Finally, in GSI development, one must consider cross reactivity to the PS-related protease SPP and its homologues (*30, 31*). In contrast, a small subset of nonsteroidal anti-inflammatory drugs (NSAIDs) has been shown to modulate γ-secretase cleavage specificity toward lowering of Aβ42 production without interfering with Notch cleavage. Modulation of γ-secretase activity by small-molecule compounds may therefore constitute a major strategic alternative for AD drug discovery (*32*), especially in light of recent findings that suggest that potent γ-secretase modulators (GSMs) can be discovered (*33*−*35*).

Discovery of GSMs or substrate-selective GSIs requires a precise understanding of the mode of action of γ-secretase, especially with respect to substrate recognition and cleavage. For example, although inhibitor and mutagenesis studies indicate the existence of a second substrate binding site (termed docking site) close to the active site (*36, 37*), it is unclear how substrates are passed from the receptor via the docking site to the active site. It will also be important to understand which factors influence the cleavage specificity of γ-secretase. Furthermore, because of the existence of two different PS (PS1 and PS2) and three different APH-1 proteins [APH-1aS (short APH-1a splice variant), APH-1aL (long APH-1a splice variant), and APH-1b], six γ-secretase complexes exist in human cells (*38, 39*), which can all principally display pathogenic activity in APP processing (*40*). It is not established whether these complexes have discrete substrate preferences. Thus, potential accessory factors involved in the selection of substrates for these complexes might exist.

Addressing these and related questions will be facilitated by the availability of significant amounts of a purified form of γ-secretase. In addition, basic questions regarding the precise subunit organization, the presence of additional components in γ-secretase complexes, and their molecular interactions are largely unresolved. Different molecular masses have been reported for γ-secretase, ranging from 250 kDa (approximately the total apparent molecular mass of the four core subunits) to 2000 kDa depending on the analytical method used (*3, 41*−*43*). Quite possibly, γ-secretase complexes either tend to oligomerize or, alternatively, contain additional components with a regulatory role, such as the recently identified CD147 (*44*) and TMP21 (*45*) and possibly others. The identification of modulatory γ-secretase subunits might be compromised when using available purification procedures that utilize cell lines overexpressing the known γ-secretase subunits (*46, 47*), as this setting could titrate out accessory proteins. Likewise, the use of epitope-tagged γ-secretase subunits in these procedures could potentially also disrupt interaction with other additional components.

To address some of these pressing questions, we therefore set out to purify and characterize endogenous γ-secretase. For the first time, we provide a fast, inexpensive, scalable, and convenient procedure for the purification of the active endogenous enzyme in considerably high grade. We furthermore validate the utility of the preparation by using pharmacological and functional proteomics means. Finally, we identify a number of copurifying proteins and provide evidence that they are unlikely to be part of the active γ-secretase enzyme.

EXPERIMENTAL PROCEDURES

Antibodies. Monoclonal and polyclonal antibodies against the PS1 N-terminus (PS1N), against the PS1 large loop (3027, APS18), against the PS2 N-terminus (BI.5D3), and against the PS2 large loop (BI.HF5c) were described previously (*41, 48*−*51*). Polyclonal antibodies against the N-terminus of PEN-2 (1638), against the third loop of APH-1aS and APH-1aL (2021), against the C-terminus of APH-1aL (433), and against the C-terminus of APH-1b (435) have been described before (*15, 39, 52*) and were used after affinity purification. Polyclonal antibody N1660 against the C-terminus of NCT was obtained from Sigma, and a monoclonal antibody to the ectodomain of NCT was from BD Biosciences. Monoclonal antibodies 6E10 against Aβ1−16

and 4G8 against Aβ17−24 were obtained from Signet laboratories and Covance Research Products, respectively. Monoclonal antibody 2D8 against Aβ1−16 and C-terminal specific antibodies to Aβ40 (BAP24), Aβ42 (BAP15), and Aβ38 (obtained from Meso Scale Discovery) were described previously (*34, 40*). Polyclonal antibody 6687 against the last 20 C-terminal amino acids of APP was described previously (*8*). The monoclonal antibody 8D6 to CD147 was obtained from Santa Cruz Biotechnology, and the polyclonal anti-NPC1 antibody (ab36983) was obtained from Abcam. Anti-TMP21 antibodies were described previously (*53*) and used after affinity purification (*45*). The anti-p24a antibody has been described previously (*45*).

Cell Lines. Human embryonic kidney 293 (HEK293) cells and HEK293 cells stably coexpressing Swedish mutant APP and PS1 wild type (wt) or PS1 L166P were cultured as described previously (*20*).

Isolation of Cell Membranes. In a typical preparation, HEK293 cells from eight confluent 10 cm dishes were washed and harvested in PBS. Cells were pooled, centrifuged for 5 min at 2500*g* at 4 °C, frozen in liquid nitrogen, and stored at −80 °C. When appropriate, cells were thawed and resuspended in 6 mL of hypotonic buffer [15 mM sodium citrate (pH 6.4), 1 mM EDTA, and 10 mM DTT] containing 1× protease inhibitors (PI) (Complete, Roche). Cells were adjusted with hypotonic buffer to an OD_{600} of 2.0 to normalize the preparations such that 0.85 mL of this suspension was defined as an equivalent of one 10 cm dish. Cells were then lysed by being frozen in liquid nitrogen for 5 min and thawed for 30 min in an ice−water bath. Following freeze−thaw lysis, Brij-35 and Lubrol WX were added to a final concentration of 1%, and incubation was continued for 20 min on ice. The resultant Brij-35/Lubrol WX lysates were then cleared by centrifugation for 30 min at 2500*g* and 4 °C. The supernatant fraction was supplemented with 5% glycerol and then subjected to ultracentrifugation for 60 min at 130000*g* and 4 °C to produce membranes enriched with γ-secretase. Membranes were thoroughly resuspended in 0.4 mL (50 μL/10 cm dish) of buffer A [50 mM BisTris-HCl (pH 7.0), 66.7 mM ε-aminocaproic acid, 5% glycerol, 1 mM EDTA, and 10 mM DTT] containing 1× PI, frozen in liquid nitrogen, and stored at −80 °C until further use.

Purification of γ-Secretase. In a typical preparation, cell membranes equivalent to eight 10 cm dishes, resuspended in buffer A containing 1× PI, were thawed and solubilized for 15 min on ice by the addition of *n*-dodecyl β-D-maltoside (DDM) to a final concentration of 0.75% and of digitonin to a final concentration 1.5%. Following a clarifying spin at 130000*g* for 40 min at 4 °C, the supernatant was mixed with an equal volume of saturated 4 M $(NH_4)_2SO_4$ to yield a final $(NH_4)_2SO_4$ concentration of 50%. The sample was incubated for 10 min on ice and then centrifuged at 16000*g* for 20 min at 4 °C. The supernatant fraction containing γ-secretase was adjusted to a $(NH_4)_2SO_4$ concentration of 75% by the addition of an equal volume of 4 M $(NH_4)_2SO_4$ and incubated for 10 min on ice, followed by the addition of water to yield a final $(NH_4)_2SO_4$ concentration of 70%. After centrifugation at 16000*g* for 30 min at 4 °C, the pellet fraction containing γ-secretase was thoroughly resuspended in 100 μL of buffer B [50 mM BisTris-HCl (pH 7.0), 66.7 mM ε-aminocaproic acid, 5% glycerol, 1 mM EDTA, 10 mM DTT, 0.1% DDM, and 0.5% digitonin] containing 55% $(NH_4)_2SO_4$ and centrifuged for 20 min at 16000*g* and 4 °C. The supernatant was mixed with 2 volumes of buffer B and wheat germ agglutinin (WGA)−agarose beads (Calbiochem) (17.5 μL, washed with 0.3 mL of water) followed by incubation in batch mode for 90 min at 4 °C with agitation. Beads were collected by centrifugation for 1 min at 9500*g* and 4 °C and washed four times with 150 μL of buffer C [5 mM sodium citrate (pH 6.4), 5% glycerol, 1 mM EDTA, 10 mM DTT, 0.1% DDM, and 0.5% digitonin] containing 300 mM methyl α-D-mannopyranoside for 5 min at 4 °C. γ-Secretase was eluted from the WGA−agarose beads with 40 μL of buffer C containing 200 mM *N*-acetylglucosamine for 20 min on ice with intermitent occasional vortexing. When the WGA−agarose eluate was used as the source of the enzyme in γ-secretase activity assays (see below), DDM and digitonin were replaced with 1% CHAPSO in the wash and elution buffers. Beads were then transferred to a 200 μL pipet tip equipped with a frit and centrifuged for 2 min at 3500*g* and 4 °C in a 1.5 mL reaction tube to yield a cleared WGA−agarose eluate by filtration. When purification was continued, the eluate was adjusted to pH 5.5 with 0.5 M acetic acid (pH 5.0) and incubated in batch mode with 25 μL of sulfopropyl (SP)-Sepharose beads, equilibrated prior to use with 0.4 mL of buffer C adjusted to pH 5.5 as described above, for 40 min at 4 °C with agitation. The SP-Sepharose beads were subjected to filtration as described above, and the flow-through fraction containing γ-secretase was neutralized by subsequent addition of 150 mM BisTris-HCl (pH 7.0), 200 mM ε-aminocaproic acid, and 0.5 M sodium borate (pH 9.0). The neutralized eluate was mixed with 5 μL of Q-Sepharose beads, equilibrated prior to use with 100 μL of buffer D [18.75 mM BisTris-HCl (pH 7.0), 25 mM ε-aminocaproic acid, 5% glycerol, 1 mM EDTA, and 10 mM DTT] containing 0.1% DDM and 0.5% digitonin, and incubated in batch mode for 90 min or O/N at 4 °C with agitation. Following centrifugation for 1 min at 9500*g* and 4 °C, beads were washed once with 100 μL of buffer D containing 1% CHAPSO and 100 mM NaCl for 5 min at 4 °C, before γ-secretase was eluted with 30 μL of buffer D containing 1% CHAPSO and 500 mM NaCl for 40 min at 4 °C with agitation. Finally, the eluate was cleared by filtration as described above. To obtain silver-stainable amounts, the preparation is scaled up 2-fold and elution from the Q-Sepharose beads is carried out with 15 μL of elution buffer. Typically, 0.1 μg of protein per 10 cm dish is obtained.

Reconstitution of γ-Secretase into Lipid Vesicles. To reconstitute γ-secretase into lipid vesicles, 1 volume of the purified enzyme preparation was diluted with 3−4 volumes of lipid vesicle-containing assay buffer [35 mM sodium citrate (pH 6.4), 3.5% glycerol, 30 mM DTT, and 0.66 mg/mL L-α-phosphatidylcholine (Sigma P3556, prepared as a 10 mg/mL sonicated stock solution) in water] and incubated with gentle shaking at 4 °C, usually O/N. For further use in γ-secretase activity assays, 1/15 of the reconstituted γ-secretase was typically used.

γ-Secretase in Vitro Assay. To assess γ-secretase activity, C100-His_6 substrate (*2*) was added to samples containing γ-secretase reconstituted with lipid vesicles. Unless indicated otherwise, C100-His_6 was typically used at concentrations of 0.25−1 μM or for determination of IC_{50} values at 1.5 μM. Where indicated, Merck A (L-685,458) GSI (*54*) or

GSMs were added at the indicated concentrations from stock solutions in DMSO. In addition to Merck A, DAPT (*55*) and compound E (*56*) were used to determine IC_{50} values from dose−response experiments. The final DMSO concentration in the assays did not exceed 4%. Samples were incubated O/N or for the indicated times at 37 °C or kept on ice as a control. Depending on the further analysis, appropriate aliquots were removed to analyze Aβ and AICD generation either by Tris-Tricine SDS−PAGE as described previously (*2*), by Tris-Bicine urea SDS−PAGE (*57*) to separate the individual Aβ species, by Aβ sandwich immunoassay to quantify Aβ species, or by mass spectrometry.

Compound Synthesis. The GSM (2*S*,4*R*)-1-[(*R*)-1-(4-chlorophenyl-4-methylpentyl)-2-(4-trifluoromethylphenyl)piperidin-4-yl]acetic acid (GSM-1) was synthesized starting from commercially available materials following the procedures described by Hannam et al. (*33*).

Colorless Native-PAGE (CN-PAGE). CN-PAGE was carried out to assess the molecular mass of the γ-secretase complex. CN-PAGE is identical to blue native-PAGE (BN-PAGE) but lacks anionic Coomassie blue dye in the sample and cathode buffer. Its application is thus restricted to proteins with a net intrinsic negative charge (*58*). In brief, purified γ-secretase was directly loaded on 7% polyacrylamide gels (from a 49.5% acrylamide/3% bisacrylamide stock) containing 50 mM BisTris-HCl (pH 7.0), 66.7 mM ε-aminocaproic acid, 20% glycerol, and 0.01% DDM. Ponceau S was added to the samples to serve as a dye front marker. Gel running buffers were 50 mM BisTris-HCl (pH 7.0) (anode buffer) and 50 mM Tricine with 15 mM BisTris (pH 7.0) (cathode buffer). Thyroglobulin (669 kDa, Sigma T9145), apoferritin (443 kDa, Sigma A3660), β-amlyase (200 kDa, Sigma A8781), and albumin (66 kDa, Sigma A8531) were dissolved at a concentration of 2 mg/mL in 50 mM BisTris-HCl (pH 7.0), 66.7 mM ε-aminocaproic acid, 5% glycerol, and 0.01% DDM and used as molecular mass markers for CN-PAGE. Following electrophoresis, gels were soaked for 5−10 min in SDS−PAGE running buffer and blotted onto a PVDF membrane for 1 h at 40 V. In the case of lipid-reconstituted γ-secretase, 0.1−0.2% DDM was added to solubilize the lipid vesicles prior to CN-PAGE.

Quantification of in Vitro-Generated Aβ and AICD. To quantify Aβ38, Aβ40, and Aβ42 species, aliquots of the γ-secretase assays were diluted with PBS containing 0.5% TX-100 and then subjected to an Aβ sandwich immunoassay, which was conducted as described previously (*34*) using biotinylated 2D8 antibody as the total Aβ capture antibody and ruthenylated antibodies specific to Aβ38, Aβ40, and Aβ42 as detection antibodies. For quantification of in vitro-generated Aβ and AICD species, the chemiluminescence signals of the respective immunoblots were quantified using the CCD camera-based FluorChem 8900 detection system (Alpha Innotech). IC_{50} values of GSIs for total Aβ inhibition were calculated from dose−response curves by nonlinear regression analysis using GraphPad Prism.

Mass Spectrometry (MS) Analysis of in Vitro-Generated Aβ and AICD Species. Following a C100-His_6 in vitro cleavage assay, samples were cleared from salt and detergent using a ZipTip (C18) according to the instructions of the manufacturer (Millipore). Bound peptides were eluted from the ZipTip with a formic acid/water/2-propanol mixture (1:4:4) saturated with α-cyano-4-hydroxycinnamic acid and subjected to MALDI-TOF MS analysis on a Voyager DE STR instrument (Applied Biosystems). Alternatively, samples were diluted with IP-MS buffer [0.1% *N*-octyl glucoside, 140 mM NaCl, and 10 mM Tris (pH 8.0)], and Aβ species were immunoprecipitated with antibody 4G8 and protein G-Sepharose for 4 h at 4 °C and then processed for MALDI-TOF MS analysis as described previously (*34*).

Tryptic Digestion and Protein Identification by LC−MS/MS. The final Q-Sepharose eluate containing γ-secretase was subjected to SDS−PAGE. Following staining of the gel with silver nitrate, visible bands were excised and the gel pieces were washed, dehydrated, reduced, and alkylated as described previously (*59*). Protein identification by LC−MS/MS was performed as outlined elsewhere (*60*). MS data were finally searched against a Cellzome-curated version of the International Protein Index (IPI), maintained at the EBI (Hinxton, U.K.). Results of database searches were read into a database system for further bioinformatics analysis.

Affinity Capture of γ-Secretase with Merck C. γ-Secretase was purified as described above except that all subsequent steps after binding to WGA−agarose beads were carried out under nonreducing conditions. Following reconstitution of the WGA−agarose eluate fraction with lipid vesicles, two aliquots of the vesicles of equal volume (100 μL) were removed. One aliquot received 0.5 μM Merck C and the other 0.5 μM Merck C and 50 μM Merck A as competitor, and the samples were incubated with gentle shaking O/N at room temperature (RT). Streptavidin−Sepharose beads (20 μL) were added, and bound γ-secretase was captured for 30 min at RT with gentle shaking. The unbound fraction was separated from the streptavidin−Sepharose beads by filtration through a pipet tip equipped with a frit. Beads containing bound γ-secretase were washed three times with mock buffer and subjected to SDS−PAGE under nonreducing conditions.

RESULTS

Purification of Active Endogenous Human γ-Secretase. To further characterize γ-secretase, we developed a purification strategy for endogenous γ-secretase from cultured mammalian cells (Figure 1A). A membrane fraction was isolated from human embryonic kidney (HEK) 293 cells, detergent-solubilized with 0.75% DDM and 1.5% digitonin, and subjected to ammonium sulfate precipitation, lectin affinity, and ion-exchange chromatography (Figure 1B−D). The purification profile of γ-secretase was monitored by immunoblotting of γ-secretase complex subunits PS1, NCT, APH-1aL, and PEN-2 (Figure 1B). In addition, we followed the presence of recently identified γ-secretase modulator components CD147 and TMP21 (Figure 1C). This profile was compared with that of the corresponding total protein, which was analyzed by direct protein staining (Figure 1D). The membrane extract was subjected to ammonium sulfate precipitation to fractionate the solubilized membrane proteins. We found that the bulk of membrane proteins were precipitated at an ammonium sulfate concentration of ~50%, whereas γ-secretase remained largely soluble under this condition. γ-Secretase was precipitated from the corresponding supernatant fraction when the ammonium sulfate concentration was increased to ~75%. Taking advantage of NCT being a glycoprotein, we subjected the γ-secretase preparation to lectin affinity chromatography using WGA−agarose

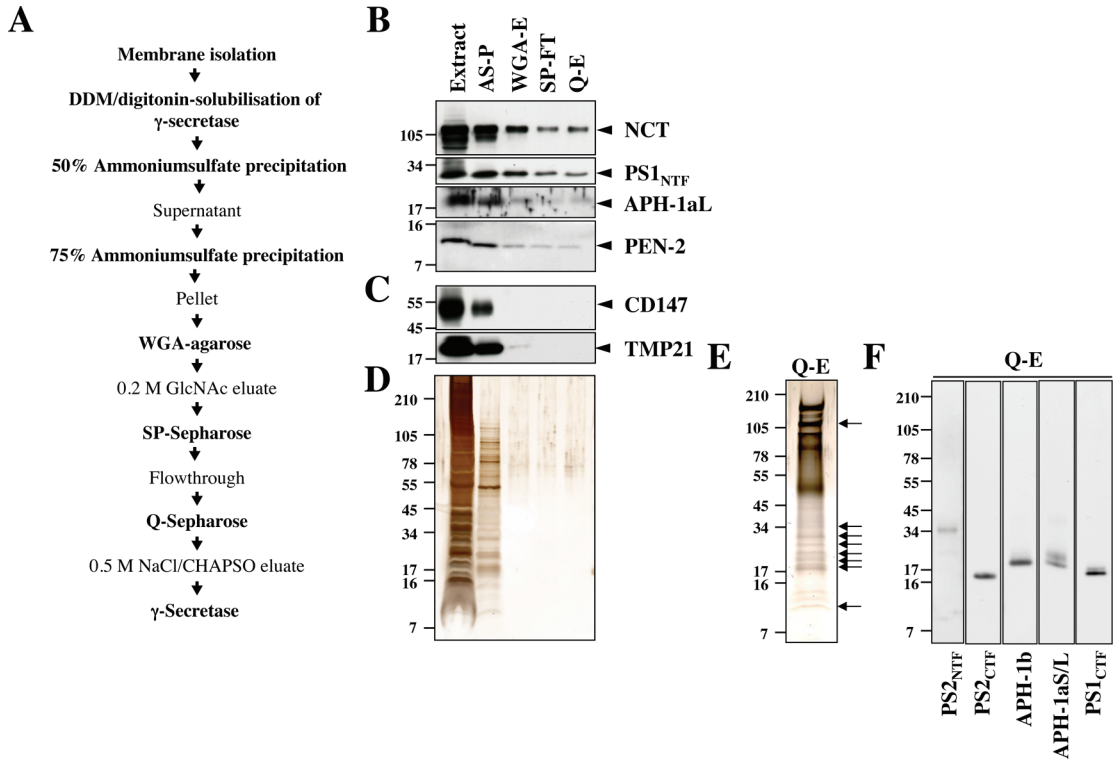

FIGURE 1: Purification of γ-secretase. (A) Overview of the γ-secretase purification scheme. (B and C) DDM/digitonin-solubilized membrane fractions of HEK293 cells were sequentially subjected to ammonium sulfate fractionation, lectin chromatography using WGA−agarose beads, and ion-exchange chromatography using SP- and Q-Sepharose. Equivalent aliquots (equal volume percentage) of each fraction were analyzed for the presence of the major γ-secretase complex containing PS1, APH-1a (as long splice variant APH-1aL), NCT, and PEN-2 by immunoblotting using antibodies N1660 (NCT), PS1N (PS1 NTF), 433 (APH-1aL), and 1638 (PEN-2) as shown in panel B and for the purification profile of γ-secretase interactors CD147 and TMP21 by immunoblotting with anti-CD147 (8D6) and anti-TMP21 antibodies (C). (D) Equivalent aliquots (equal volume percentage) of each fraction were subjected to SDS−PAGE followed by silver staining. (E) Hundred-fold larger amounts vs those shown in panel D of the Q-Sepharose eluate were subjected to SDS−PAGE and silver staining. Arrows indicate bands matching in molecular mass to γ-secretase subunits. (F) Aliquots of the last fraction were additionally analyzed for the presence of the other γ-secretase components by immunoblotting using antibodies BI.5D3 (PS2 NTF), BI.HF5c (PS2 CTF), 2021 (APH-1aS/L), 435 (APH-1b), and APS18 (PS1 CTF). AS-P, 75% ammonium sulfate precipitate; WGA-E, WGA−agarose eluate; SP-FT, SP-Sepharose flow-through; Q-E, Q-Sepharose eluate. In panels B−F, molecular mass markers are shown on the left (in kilodaltons).

beads as the next purification step. While most remaining proteins did not bind to WGA−agarose beads, a substantial fraction of γ-secretase bound and could subsequently be nearly quantitatively eluted. As shown in the following sections, these few purification steps yielded a high-grade γ-secretase preparation already sufficient for a detailed biochemical characterization. The WGA−agarose eluate could be further enriched for γ-secretase by cation-exchange chromatography using SP-Sepharose. This purification step eliminated further contaminating proteins because γ-secretase did not bind to SP-Sepharose under the condition of an operating pH of 5.5 during this chromatographic step. Finally, the SP-Sepharose flow-through fraction containing γ-secretase was adsorbed to Q-Sepharose and subsequently eluted with sodium chloride in the presence of 1% CHAPSO, a detergent that supports optimal activity of the enzyme. Comparison of the purification profiles of the core γ-secretase complex subunits (Figure 1B) with that of CD147 or TMP21 (Figure 1C) revealed that the bulk of CD147 and TMP21 was separated from γ-secretase early during purification, indicating that the vast majority of these proteins reside in γ-secretase-unrelated pools. When a large part of the Q-Sepharose eluate from a typical preparation was subjected to SDS−PAGE followed by silver staining, bands corresponding to the molecular masses of the known γ-secretase subunits were visible as well as other bands representing proteins that were copurified with γ-secretase (Figure 1E). In addition to the components already identified in Figure 1B (NCT, PS1 NTF, APH-1aL, and PEN-2), all other remaining components (PS2 NTF, PS2 CTF, APH-1b, APH-1aS, and PS1 CTF) were identified by immunoblotting (Figure 1F). Thus, all γ-secretase components were recovered in the preparation.

To assess the enzymatic activity of purified γ-secretase recovered in the last Q-Sepharose eluate fraction, the enzyme was reconstituted into lipid vesicles composed of phosphatidylcholine by dilution of CHAPSO below its critical micelle concentration. γ-Secretase activity was then assessed upon addition of the recombinant APP-based substrate C100-His_6 (purified from *E. coli*) by following the generation of the Met-Aβ and AICD-His_6 cleavage products (*2*), hereafter termed Aβ and AICD, respectively, for the sake of simplicity, via immunoblotting. The lipid-reconstituted γ-secretase exhibited robust activity, which was blocked in the presence of the γ-secretase active site transition-state analogue inhibitor Merck A (L-685,458) (*54*) (Figure 2A). Inhibitor potencies for total Aβ inhibition of Merck A and two other commonly used potent non-transition-state analogue GSIs, DAPT (*55*) and compound E (*56*), were determined in dose−response experiments (Figure 2B). The IC_{50} values calculated for Merck A (IC_{50} = 0.78 nM; log IC_{50} = −9.1 ± 0.25), DAPT (IC_{50} = 80 nM; log IC_{50} = −7.1 ± 0.27),

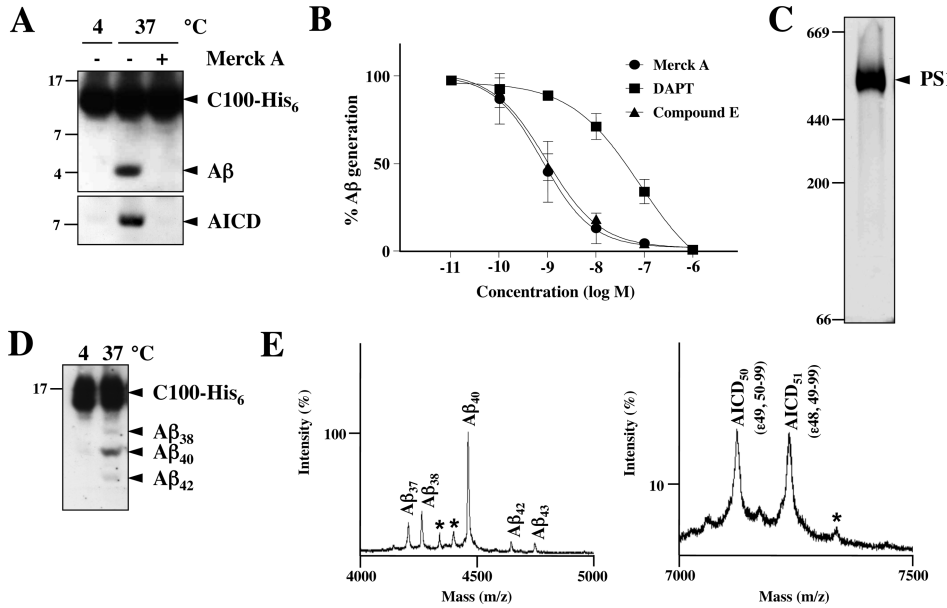

FIGURE 2: Purified γ-secretase displays authentic enzymatic properties toward an APP-based substrate. (A) Activity of purified γ-secretase reconstituted with lipids assessed using purified recombinant C100-His_6 as a substrate. γ-Secretase cleavage products of C100-His_6, Aβ and AICD, were identified by immunoblotting using antibodies 6E10 (Aβ) and 6687 (AICD). Where indicated, γ-secretase inhibitor Merck A (L-685,458) at 1 μM was present to demonstrate the specificity of C100-His_6 substrate cleavage by γ-secretase. (B) A γ-secretase activity assay was carried out as described for panel A in the presence of the indicated concentrations of Merck A, DAPT, and compound E, and the dose response of inhibition was quantified by measuring the respective Aβ signal intensities of the immunoblots of three independent experiments followed by nonlinear regression analysis. Bars represent the standard error of the mean ($n = 3$). (C) Lipid-reconstituted γ-secretase was subjected to CN-PAGE, and the PS1 γ-secretase complex was identified by immunoblotting with antibody PS1N. (D) The γ-secretase activity was assayed as described for panel A, except that Aβ species were separated by Tris-Bicine urea SDS−PAGE. Aβ38, Aβ40, and Aβ42 species were analyzed by immunoblotting with antibody 6E10. (E) A γ-secretase assay was carried out as described for panel A for 8 h at 37 °C. Following the in vitro C100-His_6 substrate cleavage reaction, Aβ and AICD species generated by purified γ-secretase were identified by direct MALDI-TOF MS analysis of the assay sample. Note that observed masses of Aβ and AICD species in the mass spectra correspond to Met-Aβ and AICD-Gly-Ser-Arg-Ser-His_6 species, respectively (*2*). Asterisks denote peaks not matching masses of Aβ or AICD species. The intensity of the Aβ40 peak was set to 100%. Absolute values of ion counts for Aβ40 and AICD were 3226 and 604, respectively. In panels A, C, and D, molecular mass markers are shown on the left (in kilodaltons).

and compound E ($IC_{50} = 0.90$ nM; $\log IC_{50} = -9.0 \pm 0.13$) were in good agreement with those reported previously for these inhibitors using recombinant APP-based C100 substrates in vitro (*43, 61*−*63*). The reconstituted enzyme was next subjected to CN-PAGE, which allows native gel electrophoresis of membrane protein complexes under milder conditions than the closely related blue native-PAGE (BN-PAGE) system (*58*). On CN-PAGE, purified γ-secretase migrated as a high-molecular mass complex of ~500 kDa (Figure 2C), consistent with the behavior of γ-secretase detergent-solubilized from membrane fractions in BN-PAGE (*16, 41, 42, 64*). Finally, we investigated whether the purified γ-secretase preparation generated authentic Aβ and AICD species. To this end, we first analyzed the generation of Aβ species by Tris-Bicine urea SDS−PAGE, which allows their electrophoretic separation (*57*). As shown in Figure 2D, purified γ-secretase generated the known individual Aβ species (Aβ38, Aβ40, and Aβ42) in physiological ratios (*19, 65, 66*). We then assessed the profile of Aβ and AICD species generated by purified γ-secretase from C100-His_6 by mass spectrometry (MS) analysis. This revealed Aβ37, Aβ38, Aβ40, Aβ42, and Aβ43 species as well as the 50- and 51-amino acid AICD species derived from the respective ε-site cleavages (*67*−*70*) (Figure 2E). Thus, purified endogenous γ-secretase displays authentic enzymatic behavior.

The specific activity of γ-secretase, as determined by the production of Aβ40 from C100-His_6 using a previously described highly sensitive and specific Aβ sandwich immunoassay (*34, 40*) as well as independently by densitometric immunoblot analysis of total Aβ, was increased in a typical preparation ~175-fold in the WGA−agarose eluate fraction and ~250-fold for the Q-Sepharose eluate fraction compared to the starting membrane extract fraction. The enrichment of γ-secretase enzyme activity correlated with the respective enrichment of PS, as determined for PS1, obtained in these fractions (i.e., the enzyme activity remained linked to PS throughout the preparation, further proving the isolation of intact γ-secretase). Because the specific γ-secretase activity was already strongly increased in the WGA−agarose eluate fraction and comparatively only moderately increased further in the Q-Sepharose eluate fraction by the additional ion-exchange steps, this fraction was taken, where described, for convenience for the further characterization of the enzyme preparation.

Pharmacological Modulation of the Cleavage Specificity of Purified γ-Secretase. It is well established that some pharmacological agents, such as a subset of NSAIDs, can modulate γ-secretase cleavage specificity (*32*). Depending on their characteristic mode of action, these γ-secretase modulators (GSMs) cause either a decrease or an increase in the amount of Aβ42 generated (*32, 71*). We therefore next investigated if the cleavage specificity of the isolated and reconstituted γ-secretase could be modulated by the potent NSAID derivative GSM-1 (*34*). Following binding to Q-Sepharose or WGA−agarose beads, γ-secretase was eluted in the presence of 1% CHAPSO and reconstituted into lipid vesicles by detergent dilution, and the enzyme activity was assessed in the presence of increasing concentrations of

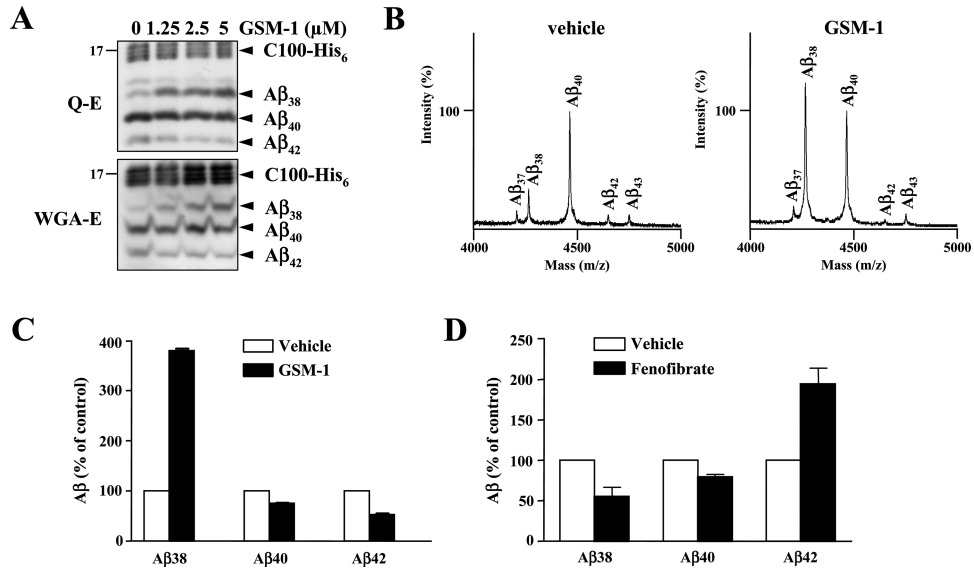

FIGURE 3: Purified γ-secretase is susceptible to γ-secretase modulators. (A) Purified γ-secretase (Q-E or WGA-E fraction) was reconstituted into lipid vesicles by detergent dilution and assessed for modulation of γ-secretase cleavage specificity using C100-His_6 substrate in the presence of increasing concentrations of GSM-1. Following separation of Aβ species by Tris-Bicine urea SDS−PAGE, samples were analyzed for Aβ38, Aβ40, and Aβ42 species by immunoblotting with antibody 6E10. Molecular mass markers are shown on the left (in kilodaltons). (B) A γ-secretase assay was conducted in the presence of 2.5 μM GSM-1 as described for panel A using γ-secretase of the WGA-E fraction as the enzyme source, and in vitro-generated Aβ species were analyzed by MALDI-TOF MS following immunoprecipitation using antibody 4G8. Note that observed masses of Aβ species in the mass spectra correspond to Met-Aβ species (*2*). The intensity of the Aβ40 peak was set to 100%. Absolute values of ion counts for Aβ40 were 1824 (vehicle) and 5490 (GSM-1). (C and D) A γ-secretase assay was carried out as described for panel B in the presence of 2.5 μM GSM-1 (C) or 150 μM fenofibrate (D). Aβ species generated were quantified from three independent experiments by a sandwich immunoassay specific for Aβ38, Aβ40, and Aβ42 species and expressed relative to the vehicle-treated control that was set to 100%. Bars represent the standard error of the mean ($n = 3$).

GSM-1 using the C100-His_6 substrate as described above. Consistent with previous results using cell-based assays and transgenic mice (*34*), GSM-1 caused a dose-dependent decrease in the level of Aβ42 and a dose-dependent increase in the level of Aβ38 (Figure 3A). Continuing the modulator experiments using the WGA−agarose eluate fraction as the enzyme source, we further confirmed the observed modulation of cleavage specificity of purified γ-secretase by GSM-1 by mass spectrometry analysis of the in vitro-generated Aβ species (Figure 3B) as well as by the Aβ sandwich immunoassay for the specific identification and quantification of the Aβ38, Aβ40, and Aβ42 species (*34, 40*) (Figure 3C). Finally, we investigated whether the inverse (Aβ42-increasing) modulator fenofibrate, a peroxisome proliferator-activated receptor α (PPARα) agonist (*71*), was effective on purified γ-secretase as well. As shown in Figure 3D, the inverse modulator fenofibrate prominently increased Aβ42 levels 2-fold as assessed by the Aβ sandwich immunoassay. In addition, this inverse modulator caused a concomitant decrease in the level of Aβ38 as well as a less pronounced decrease in the level of Aβ40 (Figure 3D). Taken together, these data show that the cleavage specificity of the purified γ-secretase can be modulated in vitro in the expected manner by mechanistically different GSMs.

Genetic Modulation of the Cleavage Specificity of Purified γ-Secretase. FAD-associated PS mutants cause a shift in the cleavage specificity of γ-secretase such that more Aβ42 and less Aβ40 are produced. This hallmark of PS FAD mutants is often associated with a reduced γ-secretase activity (*20, 72*−*77*). To address the question of whether γ-secretase isolated by our purification procedure also exhibited these characteristics, we purified the enzyme from HEK293 cells stably expressing either wt PS1 or the FAD-associated L166P mutant, one of the most aggressive FAD mutants identified to date (*20*). As such, the PS1 L166P mutant causes a strong shift in cleavage specificity and should thus allow a simple assessment of a change in cleavage specificity of purified FAD mutant γ-secretase. We found that our purification scheme could also successfully be applied to this condition of exogenous PS expression as the bulk of excess overexpressed PS holoprotein was removed by the purification procedure (Figure 4A). Thus, the purified γ-secretase contained the exogenously expressed PS as NTF and CTF; i.e., the enzyme was isolated under a quasi-endogenous condition. Purified wt and FAD mutant γ-secretase from the WGA−agarose eluate fraction were then assayed for γ-secretase activity in a time course at low C100-His_6 concentrations to facilitate the detection of substrate turnover. This revealed an overall enzyme activity of the FAD mutant lower than that of the wt enzyme (Figure 4B). As shown further in Figure 4C, the purified wt enzyme produced Aβ40 and Aβ42 at the expected ratios. Moreover, the PS1 L166P mutant enzyme generated strongly increased levels of Aβ42 and strongly reduced levels of Aβ40, as expected for this FAD mutant. Quantification confirmed that the PS1 L166P mutant was less active than wt PS1 in Aβ and AICD generation and revealed an ∼50−70% lower activity of PS1 L166P compared to the wt enzyme (Figure 4D,E). Thus, the purified PS1 L166P mutant γ-secretase exhibited both partial loss and gain of function, in agreement with previous findings (*20, 75*). Furthermore, consistent with previous results (*78, 79*), the PS1 L166P FAD mutant γ-secretase was less sensitive to Merck A treatment than wt PS1 γ-secretase (Figure 4B,C). We conclude that not only purified wt but also purified FAD mutant γ-secretase displays authentic functional characteristics analogous to those observed in living cells.

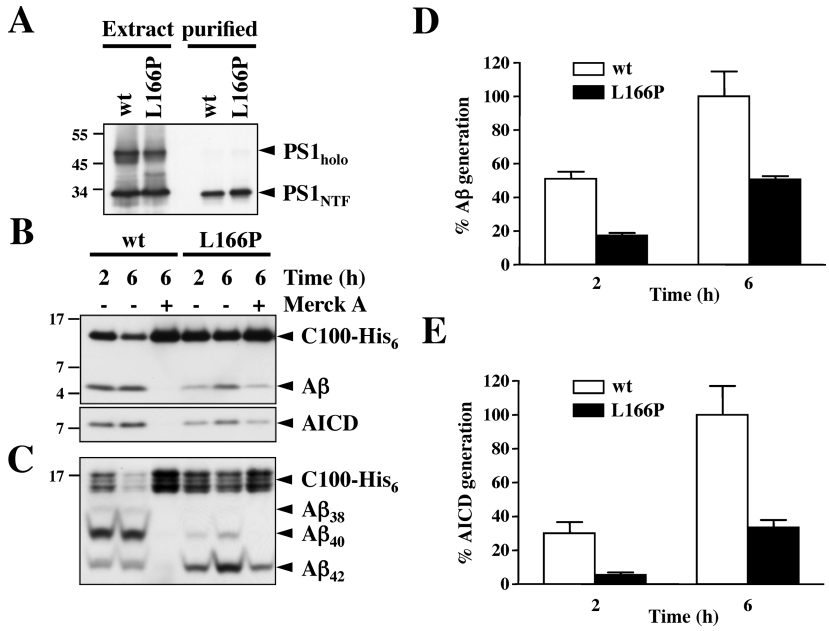

FIGURE 4: Altered cleavage specificity of purified PS1 L166P FAD mutant γ-secretase. (A) wt and FAD mutant γ-secretases were purified from HEK293 cells stably expressing wt PS1 and the PS1 L166P mutant, respectively. PS1 holoprotein and NTF in the starting membrane extract fraction and purified in the WGA-E fraction were analyzed by immunoblotting using antibody PS1N. (B and C) Purified wt and mutant γ-secretases (WGA-E fraction) were reconstituted into lipid vesicles by detergent dilution; C100-His_6 substrate (0.1 μM) was added, and the assay samples were incubated for the indicated times at 37 °C. Where indicated, Merck A inhibitor (0.5 μM) was added to the samples. The total amounts of Aβ (top panel) and AICD generated were analyzed by immunoblotting with antibodies 6E10 and 6687, respectively (B). Aliquots of the assay samples were subjected to Tris-Bicine urea SDS−PAGE and analyzed for Aβ38, Aβ40, and Aβ42 species by immunoblotting with antibody 6E10 (C). (D and E) Lipid-reconstituted purified wt and mutant γ-secretases were subjected to a γ-secretase assay for the indicated time points and analyzed as described for panel B. The production of Aβ (D) and AICD (E) was quantified by measuring the respective signal intensities at the indicated time points of the immunoblots of three independent experiments. Data are normalized to the mean value obtained for Aβ and AICD generation at the 6 h time point for PS1 wt, which was set to 100%. Bars represent the standard error of the mean ($n = 3$). In panels A−C, molecular mass markers are shown on the left (in kilodaltons).

Identification of γ-Secretase Subunits and Copurifying Proteins by Tandem Mass Spectrometry (LC−MS/MS). To confirm the presence of γ-secretase subunits in visible bands of the preparation shown in Figure 1E and to possibly identify any proteins copurifying with γ-secretase in these gel pieces, bands were cut out and trypsinized. Tryptic peptides were extracted from the gel and subjected to analysis by liquid chromatography coupled to tandem mass spectrometry (LC−MS/MS), and the presence of core γ-secretase subunits in the respective bands was demonstrated (Figure 5A). Typically, three or more independent spectra (Figure 5B) corresponding to two or more independent tryptic peptides representing the protein were identified (see the Supporting Information). For PEN-2, the masses of only two tryptic peptides fall within the mass range of detection and only one of these is typically detected. Even for PEN-2, however, we collected two independent spectra corresponding to this peptide (Figure 5B). A number of excised bands contained more than one protein, and several proteins copurifying with γ-secretase were identified (Figure 5A). In addition to γ-secretase complex core subunits PS, NCT, APH-1, and PEN-2, solute carrier family and transporter proteins (such as the ATP1A1 and ATP1B3 subunits of the sodium−potassium pump) were identified, as were proteins involved in cellular trafficking.

TMP21 and three other members of the p24 protein family, p24a, gp25aL, and p24b, were found in the preparation (Figure 5A). The latter proteins are known to form hetero-oligomeric complexes with each other and with TMP21 (*80*). The presence of CD147 in a fuzzy band of ~50 kDa was confirmed by LC−MS/MS analysis as well. Consistent with the fuzzy appearance of this band, poor electrophoretic focusing of CD147, probably caused by carbohydrate microheterogeneity, was also observed in CD147 immunoblots (see, for example, Figure 1C). Interestingly, one of the novel γ-secretase copurifying proteins identified in this study, CD98 (also termed SLC3A2 or 4F2 antigen), is a known component of the CD147 complex that has been claimed to contribute to numerous physiological processes, including the production of matrix metalloproteinases, monocyte to dendritic cell transition, and regulation of monocarboxylate transporters (*81, 82*). In the same bands as CD147, we identified the cation-dependent mannose 6-phosphate receptor (CD-M6PR), a protein that plays a key role in lysosomal protein targeting.

Finally, a major protein band of ~150 kDa was present in the silver-stained preparation (Figure 5A). LC−MS/MS analysis revealed the presence of the Niemann-Pick type C1 protein (NPC1) in this band. NPC1 is a cholesterol transport protein, which has been shown to affect γ-secretase processing of APP (*83, 84*). The identity of two other low-molecular mass proteins migrating above PEN-2 (indicated with asterisks) could not be determined possibly due to characteristics of the peptides being incompatible with LC−MS/MS.

CD147, TMP21, and NPC1 Are Not Found in Active γ-Secretase Complexes. Given the number of proteins found to be copurifying with γ-secretase in this study and in earlier ones (*44, 45*), we sought to determine whether any of these interactors were tightly associated with the active γ-secretase complex as defined by its ability to bind to an active site-directed GSI. To this end, we investigated whether purified

A

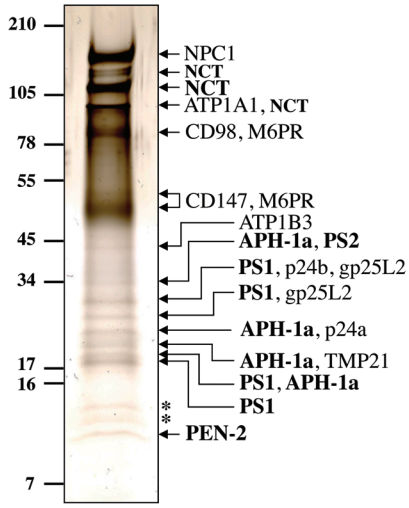

B

γ-Secretase component / co-purifying protein	Best MASCOT score	No. of matched spectra	Sequence coverage
NCT	512	30	19 %
PS1	300	10	13 %
PS2	95	3	5 %
APH-1a	189	6	8 %
PEN-2	88	2	14 %
CD147	369	12	29 %
TMP21 (p23, TMED10)	307	12	34 %
p24a (p24, TMED2)	144	6	16 %
gp25L2 (p25, TMED9)	215	7	23 %
p24b (p26, TMED4)	166	8	11 %
NPC1	1077	39	17 %
ATP1A1	2596	93	36 %
CD98 (SLC3A2, 4F2 antigen)	1277	47	43 %
M6PR	503	27	29 %
ATP1B3	184	7	15%

FIGURE 5: Identification of γ-secretase subunits and copurifying proteins by tandem mass spectrometry. (A) Visible bands of the silver-stained gel of the Q-Sepharose eluate (compare Figure 1E) were excised, digested with trypsin, and analyzed by LC−MS/MS. The asterisks indicate bands in which no proteins were identified by LC−MS/MS. Molecular mass markers are shown on the left (in kilodaltons). (B) Summary of mass spectrometric protein identification data (in case the protein was identified in multiple bands, data corresponding to the best MASCOT score are reported). For γ-secretase complex core components (bold) and copurifying proteins, short names along with the best MASCOT score, the number of independent MS/MS spectra matching the protein, and the degree of sequence coverage (see also the Supporting Information) are reported. Note also that APH-1b was identified in three of six similar experiments (best identification with 7% sequence coverage; five independent spectra; MASCOT score of 96) but not in the experiment shown here, suggesting that the amount of APH-1b present in the preparations, although readily detected by immunoblotting (Figure 1F), was near the detection limit of the MS method employed here. Another protein, podocalyxin-like protein/PODXL, was detected in several bands and appeared to smear across the entire gel lane.

γ-secretase could be affinity-captured by Merck C (*85*), a biotinylated derivative of the transition-state analogue GSI L-685,458 (Merck A). Purified γ-secretase (eluted from WGA−agarose beads) was reconstituted into lipid vesicles and incubated in the presence of Merck C alone or Merck C together with a hundred-fold excess of Merck A as a competitor to control for the specificity of affinity capture. Bound γ-secretase was isolated using streptavidin−Sepharose beads, and the specificity of the γ-secretase capture was analyzed by immunoblotting. As shown in Figure 6A, we observed highly specific binding of core complex subunits PS, NCT, APH-1, and PEN-2. In contrast, CD147, TMP21, and p24a, another p24 family member, were not coisolated with the enzyme−inhibitor complex (Figure 6B). Detection of CD147 was facilitated by using nonreducing conditions for SDS−PAGE, which, as we noticed during our studies, enhanced the immunoreactivity of CD147. Likewise, NPC1 was not captured with Merck C (Figure 6C), suggesting that these interactors are not stably associated with GSI-tractable active γ-secretase complexes.

CD147, TMP21, and NPC1 Are Present in High-Molecular Mass Complexes Distinct from γ-Secretase. Finally, to further assess a potential interaction of the cofactors of interest with γ-secretase, we subjected purified γ-secretase (eluted from WGA−agarose beads) to CN-PAGE analysis. As shown in Figure 7, CD147, TMP21, p24a, and NPC1 migrated at higher molecular masses than as monomers, suggesting that these copurifying proteins were present in the preparation as homo- or heteromeric complexes. However, CD147, TMP21, and its homologue, p24a, migrated clearly distinct from γ-secretase on CN-PAGE. Likewise, NPC1, displaying the highest molecular mass of the potential interactors on CN-PAGE, migrated separately from γ-secretase. These data suggest that γ-secretase is not stably associated with these proteins under our conditions.

DISCUSSION

A Fast, Inexpensive, and Scalable Procedure for the Purification of Endogenous γ-Secretase. Previous successful purifications of active γ-secretase have significantly advanced the field, as they enabled a more in-depth examination of the complex, such as initial structural studies (*86*), yet they have invariably made use of tagged and overexpressed variants of one or several of the four core complex subunits and/or utilized affinity resins, such as immobilized GSIs (*46*), that are expensive or not accessible to most laboratories. Purification strategies using tagged γ-secretase subunits could additionally have the drawback that the tag might potentially interfere with the interaction of other additional components. Furthermore, a potential limitation of this approach is that subunit overexpression might titrate out other candidate interaction partners such as additional nonessential, but regulatory, subunits. Indeed, the previously described γ-secretase modulators CD147 and TMP21 (*44, 45*), identified as interactors of endogenous γ-secretase that modulate APP processing, were not identified in purified overexpressed γ-secretase (*46*).

We report here a fast, reliable and convenient, scalable multistep procedure for the isolation of active endogenous γ-secretase from mammalian cells. This procedure yields a preparation that is considerably pure as judged by silver staining, that can be targeted by three classes of pharmacological agents, GSIs, GSMs, and inverse GSMs, and that

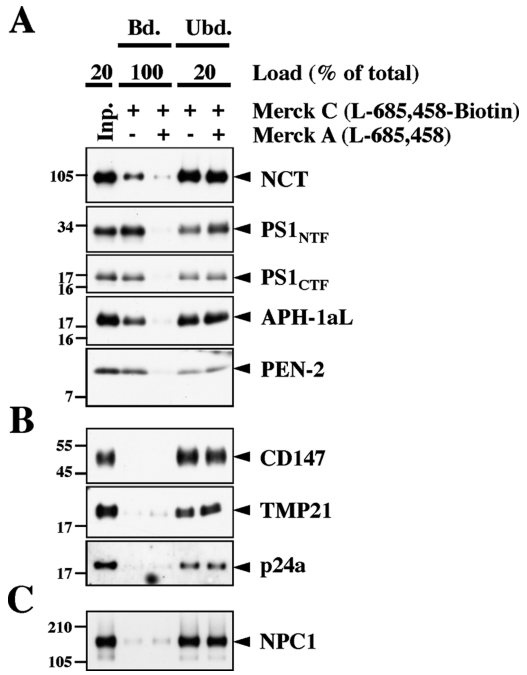

FIGURE 6: Affinity capture of γ-secretase using a biotinylated Merck C inhibitor. (A) Aliquots of purified γ-secretase were incubated with biotinylated Merck C inhibitor (0.5 μM) alone or with Merck C in the presence of 50 μM Merck A inhibitor as a competitor followed by isolation of bound proteins with streptavidin−Sepharose beads. Samples were analyzed for specific capture of the γ-secretase core subunits by immunoblotting as described for Figure 1B except that a monoclonal antibody was used for the detection of NCT and antibody 3027 for the detection of the PS1 CTF. Input and unbound material (each 20% of total) was analyzed in parallel. (B) Aliquots of the samples in panel A were analyzed for specific capture of CD147, TMP21, and p24a by immunoblotting as described for Figure 1B,C. To enhance the immunoreactivity of CD147, samples were analyzed under nonreducing conditions. (C) Aliquots of the samples in panel A were analyzed for specific capture of NPC1 by immunoblotting using antibody ab36983. In panels A−C, molecular mass markers are shown on the left (in kilodaltons).

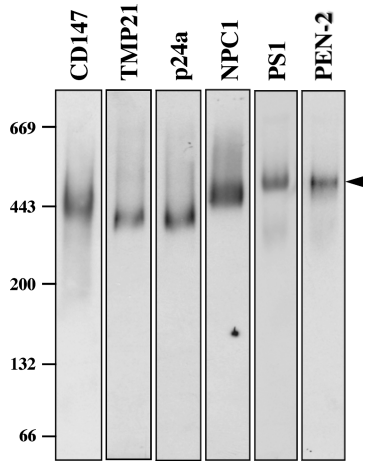

FIGURE 7: CN-PAGE analysis of γ-secretase and potential cofactors. Aliquots of the WGA-E fraction were subjected to CN-PAGE and analyzed by immunoblotting for PS1, PEN-2, CD147, and TMP21 as described for Figure 1B,C, as well as for p24a and NPC1 by immunoblotting as described in the legend of Figure 6. The arrowhead denotes γ-secretase. Molecular mass markers are shown on the left (in kilodaltons).

recapitulates the functional effects of FAD-linked mutations. It avoids the potential drawback of losing relevant γ-secretase interactors as a consequence of nonstoichiometric overexpression. The procedure presented here thus provides a powerful tool for an in-depth biochemical characterization of this pivotal AD-associated enzyme. A purification strategy in part similar to ours was used by Zhou et al. (*44*), who coisolated γ-secretase with CD147. However, Zhou et al. (*44*) did not investigate whether their preparation yielded enzymatically active γ-secretase. In addition, apart from the copurified CD147, the identity of the bands presumably representing γ-secretase subunits was not confirmed by protein sequencing or mass spectrometry.

A key step in the procedure described here to purify γ-secretase is provided by ammonium sulfate fractionation of the detergent-solubilized membrane fraction, which removes the bulk of contaminating proteins. This step is followed by lectin affinity chromatography to capture the complex via lectin binding of the highly glycosylated subunit NCT. Purification up to this step yields a γ-secretase preparation with a sufficient grade suitable for most purposes. If further purification of the enzyme complex is desired, the subsequent ion-exchange steps are carried out. In both cases, elution of bound γ-secretase from either WGA−agarose or Q−Sepharose beads then allows a convenient way for us to change from DDM and digitonin to CHAPSO to provide the optimal detergent for γ-secretase activity. Considering that the remaining copurified proteins (see below) are unlikely to be stable interaction partners of γ-secretase, the preparation is not yet purified to homogeneity.

We have successfully made larger-scale preparations, such as from 100 dishes with a 15 cm diameter ($\sim 10^9$ cells; roughly equivalent to 200 dishes with a 10 cm diameter) that have yielded $\sim$20 μg of protein from 100 mg of starting membrane extract. Even at such scale, our preparation is unable to yield γ-secretase in sufficiently large amounts (milligrams) needed for crystal structure analyses, for example. Thus, for structural studies requiring large amounts of protein, the use of purified overexpressed γ-secretase may be a complementary approach. It should be noted, however, that various cell types, including HEK293 cells used here, and HeLa, which can be adapted to growth in suspension culture, are good starting points for establishing endogenous γ-secretase purification using our method on a large scale. Finally, because exogenously expressed PS replaces endogenous PS and assembles with the other endogenous γ-secretase subunits to a functional γ-secretase complex (*20, 87*) and because we also noted that excess PS holoprotein is removed during purification, the purification procedure can be successfully applied to cell lines stably overexpressing PS.

A Validated Preparation of Endogenous γ-Secretase. An important feature of our purification procedure is that the γ-secretase enzyme isolated by this method is validated, as it displays all known biochemical characteristics. First, the purified enzyme produces Aβ38, Aβ40, and Aβ42 species in physiological ratios. The enzyme can be inhibited with well-characterized GSIs such as Merck A, DAPT, and compound E with IC_{50} values consistent with those reported previously for these inhibitors in vitro (*43, 61−63*). Second, the purified γ-secretase is susceptible to pharmacological modulation as exemplified by the effect of the Aβ42-lowering compound GSM-1. Likewise, inverse modulators exemplified by the PPARα agonist fenofibrate had the opposite, Aβ42-increasing, effect. To the best of our knowledge, this is the

first time that modulation of a purified γ-secretase by a potent GSM has been unambiguously shown. Although Fraering et al. (*46*) showed in an earlier study using purified overexpressed γ-secretase that the NSAID sulindac sulfide inhibited Aβ42 generation, there was little selectivity as the production of Aβ40 was rather strongly inhibited as well. Because the effect of sulindac sulfide on the production of Aβ38 was not investigated in this study, whether this compound actually acted as a GSM or GSI under their conditions remained unclear. Third, the cleavage specificity of purified γ-secretase containing the FAD-associated PS1 L166P mutant as the catalytic subunit is changed in the expected manner such that Aβ42 production exceeded that of Aβ40. The dramatic change in the Aβ42/Aβ40 ratio by the purified PS1 L166P mutant enzyme is highly consistent with the known behavior of this aggressive FAD mutant (*20*).

Distinguishing between Core γ-Secretase Subunits and Possible Accessory Factors. Recent advances in protein LC−MS/MS analysis have enabled the in-depth characterization of (membrane) protein complexes with increasing ease (*88*). The purification procedure described here resulted in the coisolation of two recently identified γ-secretase interactors, CD147 and TMP21 (*44, 45*), whose identity was confirmed by LC−MS/MS analysis. Our purification profile shows that most of the CD147 (like TMP21) is separated from γ-secretase early in the purification procedure, and compared to this large pool, only minor amounts are apparently copurifying with the γ-secretase core complex subunits. Surprisingly and unexpectedly from the previous report by Chen et al. (*45*), the TMP21 interactors, p24a, gp25L2, and p24b, were also copurified. Likewise, the known CD147 interactor CD98 (SLC3A2, 4F2 antigen) (*81, 82*) was copurified. This might indicate that both CD147 and TMP21 copurified as complexes and not as single subunits. Indeed, formation of a complex between TMP21 and p24a in our preparation was also suggested by chemical cross-linking (data not shown).

Given the inconsistencies between reports regarding the copurification of CD147 [identified by Zhou et al. (*44*), but not reported by Chen et al. (*45*)] and TMP21 [identified by Chen et al. (*45*), but not reported by Zhou et al. (*44*)] with γ-secretase, we tested whether they could be pulled down by Merck C, a biotinylated transition-state analogue inhibitor of γ-secretase. The observation that these proteins were not coisolated by affinity capture of γ-secretase with Merck C, i.e., using an active site-directed GSI, strongly suggests that these proteins are not cofactors of active γ-secretase complexes. Failure to capture TMP21 with Merck C was noted previously (*89*); however, because membrane extracts were used where TMP21 is in vast excess over the potentially γ-secretase-related TMP21 pool (ref *45* and Figure 1C), the significance of unsuccessful TMP21 affinity capture remained difficult to evaluate from this experimental setting. The amount of γ-secretase that we captured with Merck C inhibitor is similar to that reported by Beher et al., who developed and characterized this affinity ligand (*85*). A capture of ∼10% of PS1 by Merck C was shown to account for ∼70% of the total active γ-secretase (*85*), or more (*90*), suggesting that only a small amount of total γ-secretase is in a catalytically active conformation while the majority apparently adopts an uncapturable inactive conformation. Collectively, this suggests that we were able to capture the vast majority of active γ-secretase present in our preparation by Merck C. If, on the contrary, access to the active site was blocked by an additional subunit such as CD147 or TMP21 and if these complexes were active but not accessible with the active site-directed GSI Merck C, one could not observe a complete inhibition of γ-secretase in our preparation by the parental compound Merck A as we did. Moreover, the identification of CD147 and TMP21 as complex components that negatively regulate γ-site cleavage of APP by γ-secretase (*44, 45*) seems inconsistent with these proteins being present in active γ-secretase complexes. In agreement with these data, we did not obtain evidence of stable association of CD147 or TMP21 with γ-secretase by CN-PAGE analysis, which revealed that CD147 and TMP21 were present in high-molecular mass complexes different from that of γ-secretase. Evidence of an interaction of CD147 or TMP21 with γ-secretase could also not be provided by chemical cross-linking (data not shown). Nevertheless, while these data suggest that the vast majority of CD147 and TMP21 coisolated with γ-secretase are not stably associated with γ-secretase under our conditions, we cannot rule out the possibility that a small pool might be transiently and dynamically associated with γ-secretase. A transient interaction of these proteins with γ-secretase might possibly aid in cellular trafficking of γ-secretase itself or in proper trafficking and/or positioning of a selected substrate such as APP and/or of other γ-secretase substrate(s). It therefore seemed plausible that the lack of such an interactor could cause an alteration in Aβ production which was found for the knockdown of CD147 (*44*) or the differential effects on the cleavage of γ-secretase at the γ- and ε-sites of APP observed for the knockdown of TMP21 (*45*). With regard to CD147, a direct mode of action on γ-secretase modulating Aβ generation was however recently challenged by Vetrivel et al. (*91*), who demonstrated that CD147 rather indirectly regulates extracellular Aβ degradation. Moreover, evidence of a physical interaction of γ-secretase with CD147 could not be provided in this study (*91*). We conclude that these and our data do not support the view of CD147 as a stable γ-secretase complex component as initially reported (*44*).

Surprisingly, substantial amounts of the cholesterol transport protein NPC1 copurified with γ-secretase. NPC1 localizes to the endosomal/lysosomal compartments and is associated with Niemann-Pick type C1 disease, a rare inherited lysosomal lipid storage disorder characterized by progressive neurodegeneration. Interestingly, NPC1 has previously also been implicated in amyloidogenic processing of APP. Expression of a nonfunctional mutant NPC1 in mice and CHO cells was shown to cause increased levels of Aβ (*83, 84, 92*), a concomitant accumulation of CTFβ (*84*), and an enhanced localization of PS in endosomes (*83, 84*), suggesting that the absence of NPC1 and thus altered cholesterol transport might possibly lead to enhanced access of γ-secretase with its substrate APP. Again, the lack of stable association of NPC1 with active γ-secretase complexes captured via Merck C inhibitor affinity as well as its native molecular mass being different from that of γ-secretase suggests however that NPC1 might represent either a transient γ-secretase interactor or a copurifying contaminant remaining in the preparation. Interestingly, while this manuscript was in preparation, the purification of endogenous NPC1 using a similar purification procedure involving Q-

and SP-Sepharose ion-exchange steps was reported (*93*). Coisolation of γ-secretase with NPC1 was however not noted in this study, most likely because NP-40 was used as detergent, which does not preserve γ-secretase complex integrity. In addition to NPC1, CD-M6PR that mediates sorting of lysosomal proteins was coisolated with γ-secretase. Interestingly, it had been noted before that CD-M6PR expression was elevated in pyramidal neurons of Alzheimer brains (*94*). Moreover, overexpression of CD-M6PR led to an increased level of Aβ secretion in cultured cells (*95*). Whether the observed interaction between CD-M6PR and γ-secretase is involved in this process is at present unclear.

In summary, we provide a novel, validated, γ-secretase purification procedure, which allows the convenient and fast isolation of the active endogenous enzyme from mammalian cells. The procedure is also suitable for purifying γ-secretase from cell lines stably overexpressing PS and therefore also facilitates further biochemical analysis of γ-secretase carrying a mutant catalytic subunit.

ACKNOWLEDGMENT

We are grateful to Fusheng Chen and Peter St George-Hyslop for providing affinity-purified anti-TMP21 antibody, Felix Wieland for anti-p24a antibody, Dirk Beher and Mark Shearman for Merck C inhibitor, and Manfred Brockhaus for antibodies specific to Aβ40 and Aβ42. We thank Robert Blum and Marcus Bantscheff for helpful discussion.

SUPPORTING INFORMATION AVAILABLE

Table of peptides identified by LC−MS/MS analysis. This material is available free of charge via the Internet at http://pubs.acs.org.

REFERENCES

1. Wolfe, M. S., and Kopan, R. (2004) Intramembrane proteolysis: Theme and variations. *Science 305*, 1119–1123.
2. Edbauer, D., Winkler, E., Regula, J. T., Pesold, B., Steiner, H., and Haass, C. (2003) Reconstitution of γ-secretase activity. *Nat. Cell Biol. 5*, 486–488.
3. Kimberly, W. T., LaVoie, M. J., Ostaszewski, B. L., Ye, W., Wolfe, M. S., and Selkoe, D. J. (2003) γ-Secretase is a membrane protein complex comprised of presenilin, nicastrin, Aph-1, and Pen-2. *Proc. Natl. Acad. Sci. U.S.A. 100*, 6382–6387.
4. Takasugi, N., Tomita, T., Hayashi, I., Tsuruoka, M., Niimura, M., Takahashi, Y., Thinakaran, G., and Iwatsubo, T. (2003) The role of presenilin cofactors in the γ-secretase complex. *Nature 422*, 438–441.
5. De Strooper, B., Saftig, P., Craessaerts, K., Vanderstichele, H., Guhde, G., Annaert, W., Von Figura, K., and Van Leuven, F. (1998) Deficiency of presenilin-1 inhibits the normal cleavage of amyloid precursor protein. *Nature 391*, 387–390.
6. Wolfe, M. S., Xia, W., Ostaszewski, B. L., Diehl, T. S., Kimberly, W. T., and Selkoe, D. J. (1999) Two transmembrane aspartates in presenilin-1 required for presenilin endoproteolysis and γ-secretase activity. *Nature 398*, 513–517.
7. Steiner, H., Duff, K., Capell, A., Romig, H., Grim, M. G., Lincoln, S., Hardy, J., Yu, X., Picciano, M., Fechteler, K., Citron, M., Kopan, R., Pesold, B., Keck, S., Baader, M., Tomita, T., Iwatsubo, T., Baumeister, R., and Haass, C. (1999) A loss of function mutation of presenilin-2 interferes with amyloid β-peptide production and Notch signaling. *J. Biol. Chem. 274*, 28669–28673.
8. Steiner, H., Kostka, M., Romig, H., Basset, G., Pesold, B., Hardy, J., Capell, A., Meyn, L., Grim, M. G., Baumeister, R., Fechteler, K., and Haass, C. (2000) Glycine 384 is required for presenilin-1 function and is conserved in polytopic bacterial aspartyl proteases. *Nat. Cell Biol. 2*, 848–851.
9. Esler, W. P., Kimberly, W. T., Ostaszewski, B. L., Diehl, T. S., Moore, C. L., Tsai, J.-Y., Rahmati, T., Xia, W., Selkoe, D. J., and Wolfe, M. S. (2000) Transition-state analogue inhibitors of γ-secretase bind directly to presenilin-1. *Nat. Cell Biol. 2*, 428–433.
10. Li, Y. M., Xu, M., Lai, M. T., Huang, Q., Castro, J. L., DiMuzio-Mower, J., Harrison, T., Lellis, C., Nadin, A., Neduvelli, J. G., Register, R. B., Sardana, M. K., Shearman, M. S., Smith, A. L., Shi, X. P., Yin, K. C., Shafer, J. A., and Gardell, S. J. (2000) Photoactivated γ-secretase inhibitors directed to the active site covalently label presenilin 1. *Nature 405*, 689–694.
11. Herreman, A., Serneels, L., Annaert, W., Collen, D., Schoonjans, L., and De Strooper, B. (2000) Total inactivation of γ-secretase activity in presenilin-deficient embryonic stem cells. *Nat. Cell Biol. 2*, 461–462.
12. Zhang, Z., Nadeau, P., Song, W., Donoviel, D., Yuan, M., Bernstein, A., and Yankner, B. A. (2000) Presenilins are required for γ-secretase cleavage of βAPP and transmembrane cleavage of Notch-1. *Nat. Cell Biol. 2*, 463–465.
13. Shah, S., Lee, S. F., Tabuchi, K., Hao, Y. H., Yu, C., LaPlant, Q., Ball, H., Dann, C. E., III., Sudhof, T., and Yu, G. (2005) Nicastrin functions as a γ-secretase-substrate receptor. *Cell 122*, 435–447.
14. Lee, S. F., Shah, S., Li, H., Yu, C., Han, W., and Yu, G. (2002) Mammalian APH-1 interacts with presenilin and nicastrin and is required for intramembrane proteolysis of amyloid-β precursor protein and Notch. *J. Biol. Chem. 277*, 45013–45019.
15. Steiner, H., Winkler, E., Edbauer, D., Prokop, S., Basset, G., Yamasaki, A., Kostka, M., and Haass, C. (2002) PEN-2 is an integral component of the γ-secretase complex required for coordinated expression of presenilin and nicastrin. *J. Biol. Chem. 277*, 39062–39065.
16. Sato, T., Diehl, T. S., Narayanan, S., Funamoto, S., Ihara, Y., De Strooper, B., Steiner, H., Haass, C., and Wolfe, M. S. (2007) Active γ-secretase complexes contain only one of each component. *J. Biol. Chem. 282*, 33985–33993.
17. Parks, A. L., and Curtis, D. (2007) Presenilin diversifies its portfolio. *Trends Genet. 23*, 140–150.
18. Haass, C., and Selkoe, D. J. (2007) Soluble protein oligomers in neurodegeneration: Lessons from the Alzheimer's amyloid β-peptide. *Nat. Rev. Mol. Cell Biol. 8*, 101–112.
19. Scheuner, D., Eckman, C., Jensen, M., Song, X., Citron, M., Suzuki, N., Bird, T. D., Hardy, J., Hutton, M., Kukull, W., Larson, E., Levy-Lahad, E., Viitanen, M., Peskind, E., Poorkaj, P., Schellenberg, G., Tanzi, R., Wasco, W., Lannfelt, L., Selkoe, D., and Younkin, S. (1996) Secreted amyloid β-protein similar to that in the senile plaques of Alzheimer's disease is increased in vivo by the presenilin 1 and 2 and APP mutations linked to familial Alzheimer's disease. *Nat. Med. 2*, 864–870.
20. Moehlmann, T., Winkler, E., Xia, X., Edbauer, D., Murrell, J., Capell, A., Kaether, C., Zheng, H., Ghetti, B., Haass, C., and Steiner, H. (2002) Presenilin-1 mutations of leucine 166 equally affect the generation of the Notch and APP intracellular domains independent of their effect on Aβ42 production. *Proc. Natl. Acad. Sci. U.S.A. 99*, 8025–8030.
21. Page, R. M., Baumann, K., Tomioka, M., Perez-Revuelta, B. I., Fukumori, A., Jacobsen, H., Flohr, A., Luebbers, T., Ozmen, L., Steiner, H., and Haass, C. (2008) Generation of Aβ38 and Aβ42 is independently and differentially affected by FAD-associated presenilin 1 mutations and γ-secretase modulation. *J. Biol. Chem. 283*, 677–683.
22. Siemers, E., Skinner, M., Dean, R. A., Gonzales, C., Satterwhite, J., Farlow, M., Ness, D., and May, P. C. (2005) Safety, tolerability, and changes in amyloid β concentrations after administration of a γ-secretase inhibitor in volunteers. *Clin. Neuropharmacol. 28*, 126–132.
23. Siemers, E. R., Quinn, J. F., Kaye, J., Farlow, M. R., Porsteinsson, A., Tariot, P., Zoulnouni, P., Galvin, J. E., Holtzman, D. M., Knopman, D. S., Satterwhite, J., Gonzales, C., Dean, R. A., and May, P. C. (2006) Effects of a γ-secretase inhibitor in a randomized study of patients with Alzheimer disease. *Neurology 66*, 602–604.
24. De Strooper, B., Annaert, W., Cupers, P., Saftig, P., Craessaerts, K., Mumm, J. S., Schroeter, E. H., Schrijvers, V., Wolfe, M. S., Ray, W. J., Goate, A., and Kopan, R. (1999) A presenilin-1-dependent γ-secretase-like protease mediates release of Notch intracellular domain. *Nature 398*, 518–522.
25. Bray, S. J. (2006) Notch signalling: A simple pathway becomes complex. *Nat. Rev. Mol. Cell Biol. 7*, 678–689.
26. Searfoss, G. H., Jordan, W. H., Calligaro, D. O., Galbreath, E. J., Schirtzinger, L. M., Berridge, B. R., Gao, H., Higgins, M. A., May, P. C., and Ryan, T. P. (2003) Adipsin, a biomarker of gastrointes-

tinal toxicity mediated by a functional γ-secretase inhibitor. *J. Biol. Chem. 278*, 46107–46116.
27. Wong, G. T., Manfra, D., Poulet, F. M., Zhang, Q., Josien, H., Bara, T., Engstrom, L., Pinzon-Ortiz, M., Fine, J. S., Lee, H. J., Zhang, L., Higgins, G. A., and Parker, E. M. (2004) Chronic treatment with the γ-secretase inhibitor LY-411,575 inhibits β-amyloid peptide production and alters lymphopoiesis and intestinal cell differentiation. *J. Biol. Chem. 279*, 12876–12882.
28. Geling, A., Steiner, H., Willem, M., Bally-Cuif, L., and Haass, C. (2002) A γ-secretase inhibitor blocks Notch signaling *in vivo* and causes a severe neurogenic phenotype in zebrafish. *EMBO Rep. 3*, 688–694.
29. Best, J. D., Smith, D. W., Reilly, M. A., O'Donnell, R., Lewis, H. D., Ellis, S., Wilkie, N., Rosahl, T. W., Laroque, P. A., Boussiquet-Leroux, C., Churcher, I., Atack, J. R., Harrison, T., and Shearman, M. S. (2007) The novel γ-secretase inhibitor N-[cis-4-[(4-chlorophenyl)sulfonyl]-4-(2,5-difluorophenyl)cyclohexyl]-1,1,1-trifluoromethanesulfonamide (MRK-560) reduces amyloid plaque deposition without evidence of notch-related pathology in the Tg2576 mouse. *J. Pharmacol. Exp. Ther. 320*, 552–558.
30. Weihofen, A., Lemberg, M. K., Friedmann, E., Rueeger, H., Schmitz, A., Paganetti, P., Rovelli, G., and Martoglio, B. (2003) Targeting presenilin-type aspartic protease signal peptide peptidase with γ-secretase Inhibitors. *J. Biol. Chem. 278*, 16528–16533.
31. Iben, L. G., Olson, R. E., Balanda, L. A., Jayachandra, S., Robertson, B. J., Hay, V., Corradi, J., Prasad, C. V., Zaczek, R., Albright, C. F., and Toyn, J. H. (2007) Signal peptide peptidase and γ-secretase share equivalent inhibitor binding pharmacology. *J. Biol. Chem. 282*, 36829–36836.
32. Weggen, S., Eriksen, J. L., Das, P., Sagi, S. A., Wang, R., Pietrzik, C. U., Findlay, K. A., Smith, T. E., Murphy, M. P., Bulter, T., Kang, D. E., Marquez-Sterling, N., Golde, T. E., and Koo, E. H. (2001) A subset of NSAIDs lower amyloidogenic Aβ42 independently of cyclooxygenase activity. *Nature 414*, 212–216.
33. Hannam, J. C., Kulagowski, J. J., Madin, A., Ridgill, M. P., and Steward, E. M. (2006) International Patent WO 2006/043064.
34. Page, R. M., Baumann, K., Tomioka, M., Perez-Revuelta, B. I., Fukumori, A., Jacobsen, H., Flohr, A., Luebbers, T., Ozmen, L., Steiner, H., and Haass, C. (2008) Generation of Aβ38 and Aβ42 is independently and differentially affected by FAD-associated presenilin 1 mutations and γ-secretase modulation. *J. Biol. Chem. 283*, 677–683.
35. Cheng, S., Comer, D. D., Mao, L., Balow, G. P., and Pleynet, D. (2004) International Patent WO 2004/110350.
36. Kornilova, A. Y., Bihel, F., Das, C., and Wolfe, M. S. (2005) The initial substrate-binding site of γ-secretase is located on presenilin near the active site. *Proc. Natl. Acad. Sci. U.S.A. 102*, 3230–3235.
37. Yamasaki, A., Eimer, S., Okochi, M., Smialowska, A., Kaether, C., Baumeister, R., Haass, C., and Steiner, H. (2006) The GxGD motif of presenilin contributes to catalytic function and substrate identification of γ-secretase. *J. Neurosci. 26*, 3821–3828.
38. Hebert, S. S., Serneels, L., Dejaegere, T., Horre, K., Dabrowski, M., Baert, V., Annaert, W., Hartmann, D., and De Strooper, B. (2004) Coordinated and widespread expression of γ-secretase in vivo: Evidence for size and molecular heterogeneity. *Neurobiol. Dis. 17*, 260–272.
39. Shirotani, K., Edbauer, D., Prokop, S., Haass, C., and Steiner, H. (2004) Identification of distinct γ-secretase complexes with different APH-1 variants. *J. Biol. Chem. 279*, 41340–41345.
40. Shirotani, K., Tomioka, M., Kremmer, E., Haass, C., and Steiner, H. (2007) Pathological activity of familial Alzheimer's disease-associated mutant presenilin can be executed by six different γ-secretase complexes. *Neurobiol. Dis. 27*, 102–107.
41. Edbauer, D., Winkler, E., Haass, C., and Steiner, H. (2002) Presenilin and nicastrin regulate each other and determine amyloid β-peptide production via complex formation. *Proc. Natl. Acad. Sci. U.S.A. 99*, 8666–8671.
42. Farmery, M. R., Tjernberg, L. O., Pursglove, S. E., Bergman, A., Winblad, B., and Naslund, J. (2003) Partial purification and characterization of γ-secretase from post mortem human brain. *J. Biol. Chem. 278*, 24277–24284.
43. Li, Y. M., Lai, M. T., Xu, M., Huang, Q., DiMuzio-Mower, J., Sardana, M. K., Shi, X. P., Yin, K. C., Shafer, J. A., and Gardell, S. J. (2000) Presenilin 1 is linked with γ-secretase activity in the detergent solubilized state. *Proc. Natl. Acad. Sci. U.S.A. 97*, 6138–6143.
44. Zhou, S., Zhou, H., Walian, P. J., and Jap, B. K. (2005) CD147 is a regulatory subunit of the γ-secretase complex in Alzheimer's disease amyloid β-peptide production. *Proc. Natl. Acad. Sci. U.S.A. 102*, 7499–7504.
45. Chen, F., Hasegawa, H., Schmitt-Ulms, G., Kawarai, T., Bohm, C., Katayama, T., Gu, Y., Sanjo, N., Glista, M., Rogaeva, E., Wakutani, Y., Pardossi-Piquard, R., Ruan, X., Tandon, A., Checler, F., Marambaud, P., Hansen, K., Westaway, D., St George-Hyslop, P., and Fraser, P. (2006) TMP21 is a presenilin complex component that modulates γ-secretase but not ε-secretase activity. *Nature 440*, 1208–1212.
46. Fraering, P. C., Ye, W., Strub, J. M., Dolios, G., LaVoie, M. J., Ostaszewski, B. L., van Dorsselaer, A., Wang, R., Selkoe, D. J., and Wolfe, M. S. (2004) Purification and characterization of the human γ-secretase complex. *Biochemistry 43*, 9774–9789.
47. Cacquevel, M., Aeschbach, L., Osenkowski, P., Li, D., Ye, W., Wolfe, M. S., Li, H., Selkoe, D. J., and Fraering, P. C. (2008) Rapid purification of active γ-secretase, an intramembrane protease implicated in Alzheimer's disease. *J. Neurochem. 104*, 210–220.
48. Capell, A., Saffrich, R., Olivo, J. C., Meyn, L., Walter, J., Grünberg, J., Mathews, P., Nixon, R., Dotti, C., and Haass, C. (1997) Cellular expression and proteolytic processing of presenilin proteins is developmentally regulated during neuronal differentiation. *J. Neurochem. 69*, 2432–2440.
49. Walter, J., Grünberg, J., Capell, A., Pesold, B., Schindzielorz, A., Citron, M., Mendla, K., George-Hyslop, P. S., Multhaup, G., Selkoe, D. J., and Haass, C. (1997) Proteolytic processing of the Alzheimer disease-associated presenilin-1 generates an in vivo substrate for protein kinase C. *Proc. Natl. Acad. Sci. U.S.A. 94*, 5349–5354.
50. Capell, A., Grünberg, J., Pesold, B., Diehlmann, A., Citron, M., Nixon, R., Beyreuther, K., Selkoe, D. J., and Haass, C. (1998) The proteolytic fragments of the Alzheimer's disease-associated presenilin-1 form heterodimers and occur as a 100−150-kDa molecular mass complex. *J. Biol. Chem. 273*, 3205–3211.
51. Steiner, H., Romig, H., Grim, M. G., Philipp, U., Pesold, B., Citron, M., Baumeister, R., and Haass, C. (1999) The biological and pathological function of the presenilin-1 Δexon 9 mutation is independent of its defect to undergo proteolytic processing. *J. Biol. Chem. 274*, 7615–7618.
52. Prokop, S., Shirotani, K., Edbauer, D., Haass, C., and Steiner, H. (2004) Requirement of PEN-2 for stabilization of the presenilin NTF/CTF heterodimer within the γ-secretase complex. *J. Biol. Chem. 279*, 23255–23261.
53. Blum, R., Feick, P., Puype, M., Vandekerckhove, J., Klengel, R., Nastainczyk, W., and Schulz, I. (1996) Tmp21 and p24A, two type I proteins enriched in pancreatic microsomal membranes, are members of a protein family involved in vesicular trafficking. *J. Biol. Chem. 271*, 17183–17189.
54. Shearman, M. S., Beher, D., Clarke, E. E., Lewis, H. D., Harrison, T., Hunt, P., Nadin, A., Smith, A. L., Stevenson, G., and Castro, J. L. (2000) L-685,458, an aspartyl protease transition state mimic, is a potent inhibitor of amyloid β-protein precursor γ-secretase activity. *Biochemistry 39*, 8698–8704.
55. Dovey, H. F., John, V., Anderson, J. P., Chen, L. Z., de Saint Andrieu, P., Fang, L. Y., Freedman, S. B., Folmer, B., Goldbach, E., Holsztynska, E. J., Hu, K. L., Johnson-Wood, K. L., Kennedy, S. L., Kholodenko, D., Knops, J. E., Latimer, L. H., Lee, M., Liao, Z., Lieberburg, I. M., Motter, R. N., Mutter, L. C., Nietz, J., Quinn, K. P., Sacchi, K. L., Seubert, P. A., Shopp, G. M., Thorsett, E. D., Tung, J. S., Wu, J., Yang, S., Yin, C. T., Schenk, D. B., May, P. C., Altstiel, L. D., Bender, M. H., Boggs, L. N., Britton, T. C., Clemens, J. C., Czilli, D. L., Dieckman-McGinty, D. K., Droste, J. J., Fuson, K. S., Gitter, B. D., Hyslop, P. A., Johnstone, E. M., Li, W. Y., Little, S. P., Mabry, T. E., Miller, F. D., and Audia, J. E. (2001) Functional γ-secretase inhibitors reduce β-amyloid peptide levels in brain. *J. Neurochem. 76*, 173–181.
56. Seiffert, D., Bradley, J. D., Rominger, C. M., Rominger, D. H., Yang, F., Meredith, J. E., Jr., Wang, Q., Roach, A. H., Thompson, L. A., Spitz, S. M., Higaki, J. N., Prakash, S. R., Combs, A. P., Copeland, R. A., Arneric, S. P., Hartig, P. R., Robertson, D. W., Cordell, B., Stern, A. M., Olson, R. E., and Zaczek, R. (2000) Presenilin-1 and -2 are molecular targets for γ-secretase inhibitors. *J. Biol. Chem. 275*, 34086–34091.
57. Wiltfang, J., Smirnov, A., Schnierstein, B., Kelemen, G., Matthies, U., Klafki, H. W., Staufenbiel, M., Huther, G., Ruther, E., and Kornhuber, J. (1997) Improved electrophoretic separation and immunoblotting of β-amyloid (Aβ) peptides 1−40, 1−42, and 1−43. *Electrophoresis 18*, 527–532.
58. Schagger, H., Cramer, W. A., and von Jagow, G. (1994) Analysis of molecular masses and oligomeric states of protein complexes

by blue native electrophoresis and isolation of membrane protein complexes by two-dimensional native electrophoresis. *Anal. Biochem. 217*, 220–230.
59. Shevchenko, A., Wilm, M., Vorm, O., and Mann, M. (1996) Mass spectrometric sequencing of proteins silver-stained polyacrylamide gels. *Anal. Chem. 68*, 850–858.
60. Schirle, M., Heurtier, M. A., and Kuster, B. (2003) Profiling core proteomes of human cell lines by one-dimensional PAGE and liquid chromatography-tandem mass spectrometry. *Mol. Cell. Proteomics 2*, 1297–1305.
61. Kornilova, A. Y., Das, C., and Wolfe, M. S. (2003) Differential effects of inhibitors on the γ-secretase complex. Mechanistic implications. *J. Biol. Chem. 278*, 16470–16473.
62. Takahashi, Y., Hayashi, I., Tominari, Y., Rikimaru, K., Morohashi, Y., Kan, T., Natsugari, H., Fukuyama, T., Tomita, T., and Iwatsubo, T. (2003) Sulindac sulfide is a noncompetitive γ-secretase inhibitor that preferentially reduces Aβ42 generation. *J. Biol. Chem. 278*, 18664–18670.
63. Morohashi, Y., Kan, T., Tominari, Y., Fuwa, H., Okamura, Y., Watanabe, N., Sato, C., Natsugari, H., Fukuyama, T., Iwatsubo, T., and Tomita, T. (2006) C-Terminal fragment of presenilin is the molecular target of a dipeptidic γ-secretase-specific inhibitor DAPT (N-[N-(3,5-difluorophenacetyl)-L-alanyl]-S-phenylglycine t-butyl ester). *J. Biol. Chem. 281*, 14670–14676.
64. Nyabi, O., Bentahir, M., Horre, K., Herreman, A., Gottardi-Littell, N., Van Broeckhoven, C., Merchiers, P., Spittaels, K., Annaert, W., and De Strooper, B. (2003) Presenilins mutated at Asp257 or Asp385 restore Pen-2 expression and Nicastrin glycosylation but remain catalytically inactive in the absence of wild type Presenilin. *J. Biol. Chem. 278*, 43430–43436.
65. Vigo-Pelfrey, C., Lee, D., Keim, P., Lieberburg, I., and Schenk, D. B. (1993) Characterization of β-amyloid peptide from human cerebrospinal fluid. *J. Neurochem. 61*, 1965–1968.
66. Asami-Odaka, A., Ishibashi, Y., Kikuchi, T., Kitada, C., and Suzuki, N. (1995) Long amyloid β-protein secreted from wild-type human neuroblastoma IMR-32 cells. *Biochemistry 34*, 10272–10278.
67. Sastre, M., Steiner, H., Fuchs, K., Capell, A., Multhaup, G., Condron, M. M., Teplow, D. B., and Haass, C. (2001) Presenilin-dependent γ-secretase processing of β-amyloid precursor protein at a site corresponding to the S3 cleavage of Notch. *EMBO Rep. 2*, 835–841.
68. Weidemann, A., Eggert, S., Reinhard, F. B., Vogel, M., Paliga, K., Baier, G., Masters, C. L., Beyreuther, K., and Evin, G. (2002) A novel ε-cleavage within the transmembrane domain of the Alzheimer amyloid precursor protein demonstrates homology with Notch processing. *Biochemistry 41*, 2825–2835.
69. Gu, Y., Misonou, H., Sato, T., Dohmae, N., Takio, K., and Ihara, Y. (2001) Distinct intramembrane cleavage of the β-amyloid precursor protein family resembling γ-secretase-like cleavage of Notch. *J. Biol. Chem. 276*, 35235–35238.
70. Yu, C., Kim, S. H., Ikeuchi, T., Xu, H., Gasparini, L., Wang, R., and Sisodia, S. S. (2001) Characterization of a presenilin-mediated APP carboxyl terminal fragment CTFγ: Evidence for distinct mechanisms involved in γ-secretase processing of the APP and Notch1 transmembrane domains. *J. Biol. Chem. 276*, 43756–43760.
71. Kukar, T., Murphy, M. P., Eriksen, J. L., Sagi, S. A., Weggen, S., Smith, T. E., Ladd, T., Khan, M. A., Kache, R., Beard, J., Dodson, M., Merit, S., Ozols, V. V., Anastasiadis, P. Z., Das, P., Fauq, A., Koo, E. H., and Golde, T. E. (2005) Diverse compounds mimic Alzheimer disease-causing mutations by augmenting Aβ42 production. *Nat. Med. 11*, 545–550.
72. Song, W., Nadeau, P., Yuan, M., Yang, X., Shen, J., and Yankner, B. A. (1999) Proteolytic release and nuclear translocation of Notch-1 are induced by presenilin-1 and impaired by pathogenic presenilin-1 mutations. *Proc. Natl. Acad. Sci. U.S.A. 96*, 6959–6963.
73. Chen, F., Gu, Y., Hasegawa, H., Ruan, X., Arawaka, S., Fraser, P., Westaway, D., Mount, H., and St George-Hyslop, P. (2002) Presenilin 1 mutations activate γ42-secretase but reciprocally inhibit ε-secretase cleavage of amyloid precursor protein (APP) and S3-cleavage of notch. *J. Biol. Chem. 277*, 36521–36526.
74. Wiley, J. C., Hudson, M., Kanning, K. C., Schecterson, L. C., and Bothwell, M. (2005) Familial Alzheimer's disease mutations inhibit γ-secretase-mediated liberation of β-amyloid precursor protein carboxy-terminal fragment. *J. Neurochem. 94*, 1189–1201.
75. Bentahir, M., Nyabi, O., Verhamme, J., Tolia, A., Horre, K., Wiltfang, J., Esselmann, H., and De Strooper, B. (2006) Presenilin clinical mutations can affect γ-secretase activity by different mechanisms. *J. Neurochem. 96*, 732–742.
76. Shimojo, M., Sahara, N., Mizoroki, T., Funamoto, S., Morishima-Kawashima, M., Kudo, T., Takeda, M., Ihara, Y., Ichinose, H., and Takashima, A. (2008) Enzymatic characteristics of I213T mutant presenilin-1/γ-secretase in cell models and knock-in mouse brains: Familial Alzheimer disease-linked mutation impairs γ-site cleavage of amyloid precursor protein C-terminal fragment β. *J. Biol. Chem. 283*, 16488–16496.
77. Fluhrer, R., Fukumori, A., Martin, L., Grammer, G., Haug-Kroper, M., Klier, B., Winkler, E., Kremmer, E., Condron, M. M., Teplow, D. B., Steiner, H., and Haass, C. (2008) Intramembrane proteolysis of GxGD-type aspartyl proteases is slowed by a familial Alzheimer disease-like mutation. *J. Biol. Chem. 283*, 30121–30128.
78. Ikeuchi, T., Dolios, G., Kim, S. H., Wang, R., and Sisodia, S. S. (2003) Familial Alzheimer disease-linked presenilin 1 variants enhance production of both Aβ 1−40 and Aβ 1−42 peptides that are only partially sensitive to a potent aspartyl protease transition state inhibitor of "γ-secretase". *J. Biol. Chem. 278*, 7010–7018.
79. Czirr, E., Leuchtenberger, S., Dorner-Ciossek, C., Schneider, A., Jucker, M., Koo, E. H., Pietrzik, C. U., Baumann, K., and Weggen, S. (2007) Insensitivity to Aβ42-lowering nonsteroidal anti-inflammatory drugs and γ-secretase inhibitors is common among aggressive presenilin-1 mutations. *J. Biol. Chem. 282*, 24504–24513.
80. Jenne, N., Frey, K., Brugger, B., and Wieland, F. T. (2002) Oligomeric state and stoichiometry of p24 proteins in the early secretory pathway. *J. Biol. Chem. 277*, 46504–46511.
81. Woodhead, V. E., Binks, M. H., Chain, B. M., and Katz, D. R. (1998) From sentinel to messenger: An extended phenotypic analysis of the monocyte to dendritic cell transition. *Immunology 94*, 552–559.
82. Xu, D., and Hemler, M. E. (2005) Metabolic activation-related CD147-CD98 complex. *Mol. Cell. Proteomics 4*, 1061–1071.
83. Runz, H., Rietdorf, J., Tomic, I., de Bernard, M., Beyreuther, K., Pepperkok, R., and Hartmann, T. (2002) Inhibition of intracellular cholesterol transport alters presenilin localization and amyloid precursor protein processing in neuronal cells. *J. Neurosci. 22*, 1679–1689.
84. Burns, M., Gaynor, K., Olm, V., Mercken, M., LaFrancois, J., Wang, L., Mathews, P. M., Noble, W., Matsuoka, Y., and Duff, K. (2003) Presenilin redistribution associated with aberrant cholesterol transport enhances β-amyloid production in vivo. *J. Neurosci. 23*, 5645–5649.
85. Beher, D., Fricker, M., Nadin, A., Clarke, E. E., Wrigley, J. D., Li, Y. M., Culvenor, J. G., Masters, C. L., Harrison, T., and Shearman, M. S. (2003) In vitro characterization of the presenilin-dependent γ-secretase complex using a novel affinity ligand. *Biochemistry 42*, 8133–8142.
86. Lazarov, V. K., Fraering, P. C., Ye, W., Wolfe, M. S., Selkoe, D. J., and Li, H. (2006) Electron microscopic structure of purified, active γ-secretase reveals an aqueous intramembrane chamber and two pores. *Proc. Natl. Acad. Sci. U.S.A. 103*, 6889–6894.
87. Thinakaran, G., Harris, C. L., Ratovitski, T., Davenport, F., Slunt, H. H., Price, D. L., Borchelt, D. R., and Sisodia, S. S. (1997) Evidence that levels of presenilins (PS1 and PS2) are coordinately regulated by competition for limiting cellular factors. *J. Biol. Chem. 272*, 28415–28422.
88. Hopf, C., Bantscheff, M., and Drewes, G. (2007) Pathway proteomics and chemical proteomics team up in drug discovery. *Neurodegener. Dis. 4*, 270–280.
89. Vetrivel, K. S., Gong, P., Bowen, J. W., Cheng, H., Chen, Y., Carter, M., Nguyen, P. D., Placanica, L., Wieland, F. T., Li, Y. M., Kounnas, M. Z., and Thinakaran, G. (2007) Dual roles of the transmembrane protein p23/TMP21 in the modulation of amyloid precursor protein metabolism. *Mol. Neurodegener. 2*, 4.
90. Capell, A., Beher, D., Prokop, S., Steiner, H., Kaether, C., Shearman, M. S., and Haass, C. (2005) γ-Secretase complex assembly within the early secretory pathway. *J. Biol. Chem. 280*, 6471–6478.
91. Vetrivel, K. S., Zhang, X., Meckler, X., Cheng, H., Lee, S., Gong, P., Lopes, K. O., Chen, Y., Iwata, N., Yin, K. J., Lee, J. M., Parent, A. T., Saido, T. C., Li, Y. M., Sisodia, S. S., and Thinakaran, G. (2008) Evidence that CD147 modulation of β-amyloid (Aβ) levels is mediated by extracellular degradation of secreted Aβ. *J. Biol. Chem. 283*, 19489–19498.
92. Yamazaki, T., Chang, T. Y., Haass, C., and Ihara, Y. (2001) Accumulation and aggregation of amyloid β-protein in late endosomes of Niemann-pick type C cells. *J. Biol. Chem. 276*, 4454–4460.
93. Infante, R. E., Abi-Mosleh, L., Radhakrishnan, A., Dale, J. D., Brown, M. S., and Goldstein, J. L. (2008) Purified NPC1 Protein:

I. Binding of cholesterol and oxysterols to a 1278-amino acid membrane protein. *J. Biol. Chem. 283*, 1052–1063.
94. Cataldo, A. M., Barnett, J. L., Pieroni, C., and Nixon, R. A. (1997) Increased neuronal endocytosis and protease delivery to early endosomes in sporadic Alzheimer's disease: Neuropathologic evidence for a mechanism of increased β-amyloidogenesis. *J. Neurosci. 17*, 6142–6151.
95. Mathews, P. M., Guerra, C. B., Jiang, Y., Grbovic, O. M., Kao, B. H., Schmidt, S. D., Dinakar, R., Mercken, M., Hille-Rehfeld, A., Rohrer, J., Mehta, P., Cataldo, A. M., and Nixon, R. A. (2002) Alzheimer's disease-related overexpression of the cation-dependent mannose 6-phosphate receptor increases Aβ secretion: Role for altered lysosomal hydrolase distribution in β-amyloidogenesis. *J. Biol. Chem. 277*, 5299–5307.

BI801204G